ABRUPT FAULT DETECTION AND ACCOMMODATION FOR AIR DATA SYSTEMS

A THESIS SUBMITTED TO
THE GRADUATE SCHOOL OF NATURAL AND APPLIED SCIENCES
OF
MIDDLE EAST TECHNICAL UNIVERSITY

BY

SEMA KARAHAN

IN PARTIAL FULFILLMENT OF THE REQUIREMENTS
FOR
THE DEGREE OF MASTER OF SCIENCE
IN
AEROSPACE ENGINEERING

FEBRUARY 2016

Approval of the thesis:

ABRUPT FAULT DETECTION AND ACCOMMODATION FOR AIR DATA SYSTEMS

submitted by **SEMA KARAHAN** in partial fulfillment of the requirements for the degree of **Master of Science in Aerospace Engineering Department, Middle East Technical University** by,

Prof. Dr. Gülbin Dural Ünver
Dean, Graduate School of **Natural and Applied Sciences** _____

Prof. Dr. Ozan Tekinalp
Head of Department, **Aerospace Engineering** _____

Assist. Prof. Dr. Ali Türker Kutay
Supervisor, **Aerospace Engineering Dept., METU** _____

Examining Committee Members:

Prof. Dr. Ozan Tekinalp
Aerospace Engineering Department, METU _____

Assist. Prof. Dr. Ali Türker Kutay
Aerospace Engineering Department, METU _____

Prof. Dr. Ünver Kaynak
Mechanical Engineering Department, TOBB _____

Prof. Dr. Kemal Leblebicioğlu
Electrical and Electronics Engineering Department, METU _____

Assoc. Prof. Dr. İlkay Yavrucuk
Aerospace Engineering Department, METU _____

Date: _____

I hereby declare that all information in this document has been obtained and presented in accordance with academic rules and ethical conduct. I also declare that, as required by these rules and conduct, I have fully cited and referenced all material and results that are not original to this work.

Name, Last Name: SEMA KARAHAN

Signature :

ABSTRACT

ABRUPT FAULT DETECTION AND ACCOMMODATION FOR AIR DATA SYSTEMS

Karahan, Sema

M.S., Department of Aerospace Engineering

Supervisor : Assist. Prof. Dr. Ali Türker Kutay

February 2016, 82 pages

The aim of this thesis is to design a fault detection and accommodation (FDA) algorithm for air data systems, and offer a new calibration algorithm for five-hole probes (5hp) that can tolerate one port blockage and continues to give correct data.

Air data systems use 5hp to measure the magnitude and direction of airspeed. However, five-hole probes are very vulnerable to obstruction. Numerous fatal accidents happened because of probe blockages. Hardware redundancy is applied as a precaution for air data system failures, but this does not provide a solution against common-mode failures. Analytical redundancy arises as a solution, and different methods have been utilized for FDA. In these methods, wind data estimation is critical for the detection performance. Wind data are either taken from another source or estimated. In the scope of this thesis, a signal based fault detection system that does not require any wind data input is developed. Then,

a model based fault accommodation algorithm is implemented. The algorithm is tested under various wind and turbulence conditions. At each trial fault is detected within 0.5 seconds, and accommodated.

Current calibration algorithms for 5hp do not allow the isolation of a faulty port reading, and even if one port is blocked, they fail to give correct outputs. Contrarily, the new calibration algorithm eliminates the erroneous data from the algorithm, and continues with healthy data. This approach enhances the operating conditions of 5hp.

Keywords: fault detection and accommodation, five-hole probe, calibration, analytical redundancy, air data system

ÖZ

UÇUŞ VERİ SİSTEMLERİ İÇİN ANİ ARIZA BULGULAMA VE İKAME

Karahan, Sema
Yüksek Lisans, Havacılık ve Uzay Mühendisliği Bölümü
Tez Yöneticisi : Yrd. Doç. Dr. Ali Türker Kutay

Şubat 2016 , 82 sayfa

Bu tezin amacı, uçuş veri sistemleri için arıza bulgulama ve ikame sistemi geliştirilmesi ve beş delikli problar için tek port tıkanıklığını tolere edip doğru data vermelerini sağlayacak yeni bir algoritma sunulmasıdır.

Uçuş veri sistemleri hava hızının büyüklük ve yönünü ölçmek için beş delikli prob kullanmaktadır. Ancak beş delikli problar tıkanıklıklara karşı hassastır. Prob tıkanıklığının yol açtığı pek çok ölümcül kaza olmuştur. Donanımsal yedeklilik tedbir olarak uygulanmaktadır ancak bu tedbir ortak mod hatalarına karşı bir çözüm sunamamaktadır. Analitik yedeklilik bu noktada çözüm olarak ortaya çıkmaktadır ve arıza bulgulama-ikame için farklı metotlar kullanılmıştır. Bu metotlarda, rüzgar datasının tahmin edilmesi arıza bulgulama performansı için krtik önem arz etmektedir. Rüzgar verisi ya başka bir kaynaktan alınmakta ya da tahmin edilmektedir. Bu tez kapsamında, rüzgar datasına gereksinim duymayan sinyal tabanlı bir arıza bulgulama sistemi geliştirilmiştir. Ardından model tabanlı bir arıza ikame algoritması uygulanmıştır. Algoritma farklı rüzgar

ve türbülans koşullarında test edilmiştir. Her seferinde 0.5 saniye içerisinde hata bulgulanmış ve ikame edilmiştir.

Beş delikli problar için mevcut kalibrasyon algoritmaları hatalı bir port okumasını izole edememekte ve tek bir port bile tıkansa hatalı sonuç vermektedir. Buna karşılık yeni kalibrasyon algoritması hatalı port datasını algoritmadan çıkararak sağlıklı verilerle çalışmaya devam etmektedir. Bu yaklaşım beş delikli probların çalışma şartlarını genişletmektedir.

Anahtar Kelimeler: arıza bulgulama ve ikame, 5 delikli prob, kalibrasyon, analitik yedeklilik, uçuş veri sistemi

To my family

ACKNOWLEDGMENTS

I would like to thank my supervisor Asst. Prof. Dr. Ali Türker KUTAY for his guidance and support throughout the M.Sc. study.

I would like to express my appreciation to Prof. Dr. Gözde Bozdağı AKAR and Prof. Dr. Çağatay CANDAN for their valuable ideas and guidance.

Finally, I would like to express my sincere thanks to my family for their endless love and support.

TABLE OF CONTENTS

APPENDICES

LIST OF TABLES

TABLES

LIST OF FIGURES

FIGURES

LIST OF ABBREVIATIONS

α	Angle of attack
β	Angle of sideslip
M	Mach number
C_α	Angle of attack coefficient
C_β	Angle of sideslip coefficient
C_M	Mach number coefficient
C_{1-4}	Port coefficients
C_{av}	Average pressure coefficient
P_{1-6}	Pressure port readings
P_{av}	Average of the side ports(1-2-3-4) pressure readings

CHAPTER 1

INTRODUCTION

1.1 Background and Motivation

Air data systems (ADS) are used to measure airspeed, flight angles and altitude. An air data system contains a pitot tube or five-hole probe sensor. The outputs of air data system are of utmost importance for flight control. Measured dynamic pressure is used to calculate Calibrated Air Speed (CAS). CAS indicates the dynamic pressure acting on aircraft surfaces, and flight control depends on CAS. Airspeed data is also used in altitude corrections. Altitude of an aircraft is calculated from local static pressure which is measured by static pressure ports located on aircraft fuselage or pitot probe. Due to the body effect of aircraft, measured static pressure differs from the freestream static pressure. The difference between local and freestream static pressure is obtained as a function of airspeed (Mach) for correction purposes. During the flight, measured static pressure is corrected via airspeed, and true altitude is found. On the other hand, depending on the aerodynamic characteristics of aircraft, the threshold of the stall warning may change with Mach number. Hence, airspeed is also used to set stall warnings.

The only sensor that measures airspeed is air data system. Unfortunately, this critical sensor is very vulnerable to environmental effects. Since it is exposed to the incoming flow, small particals such as dust, ice can easily block the ports and cause erroneous air data measurements. In the past, a lot of accidents with fatal consequences happened because of pitot tube/five-hole probe obstruction .

1.1.1 Air Data System Failure Related Accidents

A list of pitot-tube failure related accidents[1] is given in Table 1.1. Pitot tube icing during the flight and port blockage before the take off are prominent reasons for the failures. Some of them are explained below.

Austral Líneas Aéreas Flight 2553, 1997 : A McDonnell Douglas DC-9-32 crashed on the lands of Estancia Magallanes, Uruguay, on 10 October 1997. During the flight, the aircraft's airspeed indicator began to decrease alarmingly. This case was interpreted as a loss of engine power by the pilots and they increased the power to maintain the speed. However, airspeed was indicated erroneously low because of ice accumulation inside the pitot tube and true airspeed was higher than the indicated. Pilot's reaction increased the airspeed dangerously and caused structural damage. The aircraft soon became uncontrollable and crashed. All 74 passengers and crew died. [2]

Birgenair Flight 301,1999 : Birgenair Flight 301 crashed shortly after take off from Puerto Plata in the Dominican Republic on 6 February 1996, killing 189 occupants [3]. Air speed indicator was not working properly. While the plane was climbing through 4,700 feet (1,400 m) with 220 knots, the erroneous airspeed indicator read 350 knots (650 km/h). The autopilot, which was taking its air speed information from the erroneous airspeed indicator, increased the pitch-up attitude and lowered the airplane's speed. The airplane, Boeing 757–225 stalled and crashed in to the sea off the northern coast of the Dominican Republic. The investigators reported that faulty airspeed indication was caused by a blocked pitot tube[4, 5].

Air France Flight 447, 2009 : Air France Flight 447 was a passenger flight from Rio de Janeiro, Brazil to Paris, France, which crashed into the Atlantic Ocean on 1 June 2009, killing all 228 occupants. The airplane, Airbus A330-203 stalled and could not be recovered [6]. It was reported that pitot probes were blocked by ice crystals during the cruise. Pitot tube failure occured 3 minutes before the crash and resulted in inconsistent airspeed data and autopilot disengagement. 3 pitot tubes were used and heated electrically to protect them from icing.

Table1.1: Air Data System Failure Related Accidents

Airline	Date	Location	Aircraft	Cause of accident
Scandanavian Airlines Flight 630	30 Jan 1973	Oslo-Fornebu Airport (FBU)	McDonnell Douglas DC-9	Pitot tube was blocked by ice crystals
Northwest Airlines Flight 6231	1 Dec 1974	Stoney Point, New York	Boeing 727	Pitot tube was blocked by ice crystals
Florida Commuter Airlines Flight 65	12 Sep 1980	Atlantic Ocean near Grand Bahama Island	DC-3A	Pitot tube was blocked by mud dauber nest
Air Florida Flight 90	13 Jan 1982	Washington National Airport, Washington, D.C	Boeing 737-200	Pitot tube was blocked by ice crystals
Panorama Flight Service	28 Jul 1984	Waterville-Robert Lafleur Airport, ME (WVL)	Learjet 25B	Pitot covers were not removed before the flight
Aeroflot	21 May 1986	Approach to Moscow Airport	Tupolev 154B	Pitot tube was blocked by ice crystals
Continental Airlines Flight 795	2 Mar 1994	New York - LaGuardia (LGA)	McDonnell Douglas MD-82	Pitot tube was blocked by ice crystals
Birgenair Flight 301	6 Feb 1996	Atlantic Ocean	Boeing 757–225	Pitot tube was blocked by mud dauber nest
Aero Peru Flight 603	2 Oct 1996	Lima, Peru (LIM)	Boeing 757	Pitot covers were not removed before the flight
Turkish Airlines Flight 5904	7 Apr 1999	Adana, Turkey	Boeing 737	Pitot tube was blocked by ice crystals
FedEx Flight 87	17 Oct 1999	Subic Bay Airport, Phillipines	McDonnell Douglas MD-11	Pitot drain was clogged
Air France 447	1 Jun 2009	Central Atlantic Ocean	Airbus A330	Pitot tube was blocked by ice crystals
Etihad Airways	13 Nov 2013	Brisbane Airport, Australia	Airbus A330	Pitot tube was blocked by mud dauber nest

Investigations did not reveal any malfunction of the heaters. However, for severe conditions, when the concentration of ice crystals is greater than the capacity for de-icing of the heating unit, it might take 1 to 2 minutes to de-ice and start to function properly again [7]. Details and flight data of Air France 447 accident is given in Chapter 4 .

Ghana International Airlines, 2009: On 28 January 2009, a Boeing 757-200 being operated by Astraeus AL for Ghana Airways experienced a pitot tube blockage too. Flight Management Computer used the blocked pitot tube for airspeed input. Since the blocked pitot indicated airspeed higher than the true airspeed, a false overspeed alarm was given and followed by a pitch-up maneuver by autopilot which stalled the aircraft. The flight crew was able to recover from the stall and return safely. After the flight, remains of a beetle-like creature were found in the left hand pitot tube [8].

1.1.2 Measures Against Air Data System Failure

Some precautions are taken by the industry against pitot tube/ 5hp blockage and icing. All the pitot tubes incorporate heaters that are used to prevent ice accumulation. However, heater system may fail due to a short circuit, or if the concentration of ice crystals is greater than the capacity for de-icing of the heater, ice crystals accumulate and the pitot tube is blocked. In general, around 1 or 2 minutes of heating de-ice the accumulated crystals, and pitot tube starts to function again[7].

Additionally, hardware redundancy is used to improve safety. Extra probes are installed and in case a probe fails, it is expected to have data from the other probes. A voting scheme with majority principle is used to determine the correct data. However, all the redundant probes are exposed to the same environmental conditions. As in the case of Air France Flight 447, when one probe fails, there is a high probability that the others will fail as well. Hardware redundancy does not provide any solution to this type of common mode failures. In commercial aircrafts, when there exists a mismatch within the redundant probe outputs and no majority is reached, autopilot disengages automatically and the pilot takes

the control to handle the situation. However, the pilot is left with no reliable data and it is possible for him/her to act inadequately.

Silva and Nicholson [9] investigated the accidents and incidents caused by unreliable airspeed indication. Figure 1.1.2 shows the breakdown of problems. It shows that inappropriate responses of flight crew could bring fatal consequences. A simulation of AF-447 accident scenario is conducted by investigators. Figure 1.1.2 shows flight data recorder parameters and simulated accident scenarios with and without pilot inputs. It shows that if there were no pilot inputs, the aircraft would not stall.

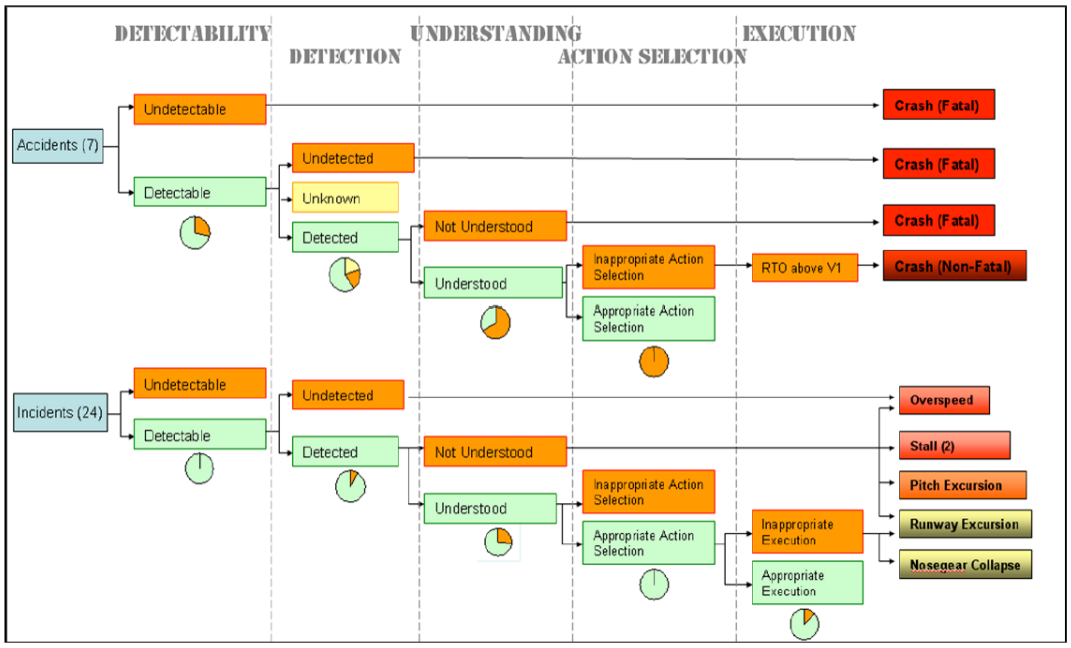

Figure 1.1: Breakdown of unreliable airspeed events-Sathya S. Silva, Roger K. Nicholson,"Categorization of Unreliable Airspeed Events Using Rasmussen's Human Performance Model",2012

Hardware redundancy and current approaches could not provide enough safety for air data system failures. Analytical redundancy is sought for an alternative solution to this burden. Diversity is introduced to avoid common mode failures. Since there exist no alternative sensor for air data measurement, a virtual sensor is generated with the help of analytical relations. Measurements of the other sensors are converted into air data via kinematic and dynamic rela-

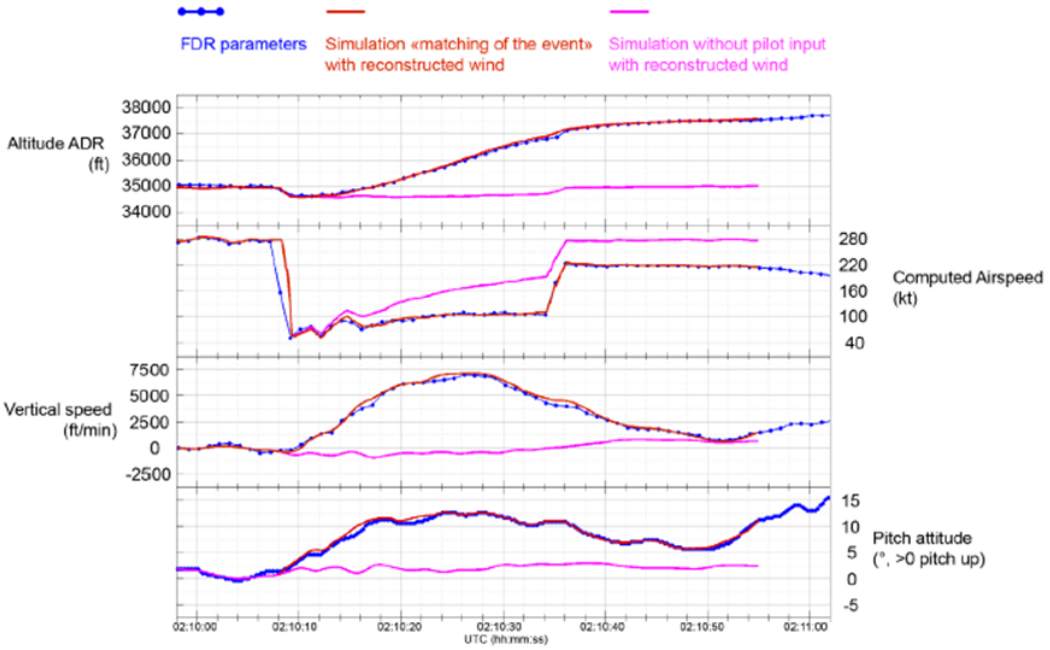

Figure 1.2: AF447-Comparison between recorded parameters and the simulation-BEA, "Final Report: On the accident on 1st June 2009 to the Airbus A330-203 registered F-GZCP operated by Air France flight AF 447 Rio de Janeiro - Paris",2012

tionships. Researchers have been working on this over decades, and in the last decade industry also has paid more attention to this field[10]. Projects like ESA SMART-FDIR, European projects ADDSAFE and some NASA SBIR programs focus on analytical redundancy.

Another aspect for analytical redundancy implementations is to reduce weight to obtain greener aircraft. For future applications, it is aimed to reduce redundant hardwares as much as possible and to obtain light-weight, fuel efficient aircrafts. Also, for small uavs it is not feasible to add extra sensors because of size and weight limitations. Analytical approach provides solutions in this case as well.

1.2 Objective

The aim of this study is to develop a fault detection and accommodation (FDA) system for air data systems and offer a new calibration algorithm for 5hp that can tolerate one port blockage and continues to give correct data. Numerous fault detection methods have been utilized for air data systems. In these methods, wind data are required and critical for the detection performance. In the scope this thesis, a signal based fault detection algorithm that does not require any wind data is developed. Also, current calibration algorithms do not allow the isolation of a faulty port reading and even if one port is blocked, they fail to give correct outputs. A new calibration algorithm is proposed to enhance the operating regions of 5hp.

1.3 Thesis Outline

The outline of this thesis is arranged as follows:

In Chapter 2, a literature review is presented on fault detection and accommodation systems used in aerospace industry.

In Chapter 3, five-hole probe working principle and calibration methods are explained. The new calibration algorithm which enhances the operating range of five-hole probe is described and compared with the traditional calibration methods.

Chapter 4 Air France 447 accident data are studied. Consequences of a port blockage are investigated.

In Chapter 5, fault detection and accommodation methods used in the study are explained in detail. Also the simulation environment in which the methods were studied is explained.

Chapter 6 gives the simulation results of the fault detection and accommodation algorithm for various scenarios.

Chapter7 presents some concluding remarks and future studies.

CHAPTER 2

LITERATURE REVIEW

2.1 Fault Detection and Accommodation

According to IFAC Technical Committee SAFEPROCESS, a fault is defined as "an unpermitted deviation of at least one characteristic property or parameter of the system from the acceptable / usual / standard condition". "Determination of the faults present in a system and the time of detection" is called fault detection(FD)[11]. Fault accommodation is the replacement of faulty data with healthy ones. Early detection and correction of faults can avoid fatal accidents and severe failures.

A fault detection system should be sensitive to faults and insensitive to noise and disturbances.[12, 13]. Performance criteria for fault detection systems are given as: [14, 10]

- Rate of missed alarms that system does not indicate any fault when a fault exists.
- Rate of false alarms that system indicates fault in a fault-free condition
- Detection delay, which is the difference between the fault occurance and fault detection time.

The time-behaviour of a fault must be considered during the FD system design. It effects the sensitivity and performance of FD system. The time-behaviour of a fault is classified as:[15]

- abrupt fault (stepwise)
- incipient fault (drift-like,gradual)
- intermittent fault.

On the other hand, in terms of their effects on the system parts, faults are grouped under three categories:[16]

- Sensor fault, which results in anomalous variation in measurements.
- Actuator fault, which leads to malfunction on a device
- Process fault, which caused by unexpected changes in the system parameters

Depending on the type of fault, different precautions and FD algorithms are introduced into the system. Since the focus of this study is on the air data system faults, sensor faults were studied. Interested readers may refer to [16] for the other types.

Although different fault detection approaches exist in the literature, generally they consist of two main tasks: residual generation and residual evaluation. In residual generation, reference quantities are obtained for measurable variables of the system. Depending on the methodology applied, reference quantities may be obtained in different ways, i.e. they might be the outputs of a redundant sensor or a mathematical model. The difference between references and measurements are taken as residuals. These residuals are used for health monitoring of the system. Residuals should be close to zero during the fault-free conditions. On the other hand, they should change significantly and become noticeable when fault occurs[16, 17]. For the residual evaluation, residual signals are processed with pre-set decision rules to determine whether a fault is occured or not. The core idea of residual evaluation is to set a threshold. When residual exceeds this threshold a fault alarm is given. The threshold setting effects false alarm rate, missed alarm rate and detection delay directly.

A simple approach for threshold selection is setting a static limit. Upper and lower limits must be large enough and compensate model uncertainties and disturbances to avoid false alarms. Thus, small errors may not be detected with this method. An alternative approach is to set an adaptive threshold that will be arranged according to the measured signal [18]. Upper and lower bound are determined online, and are updated according to the signal trend. This approach reduces the rate of false alarms and detection time.

2.2 Fault Detection and Accommodation for Air Data Systems

It is of utmost importance to have reliable measurements for flight safety. Undetected failures mislead autopilot and flight crew in a catastrophic way. There have been numerous accidents caused by unreliable air data readings. A great deal of countermeasures to air data failures have been proposed by industry and academy. There exist two main methods; hardware redundancy and analytical redundancy.

2.2.1 Hardware Redundancy

The standard industrial practice against sensor failures is hardware redundancy[19]. Additional sensors are installed to improve reliability. Commercial aircrafts are equipped with at least 3 air data systems [20]. Two alternative methods exist for hardware redundancy; static redundancy and dynamic redundancy [21]. In static redundancy, three or more hardwares are used and their outputs are evaluated by a voter system. The correct output is determined due to majority principle. In dynamic redundancy, one hardware is in service while one or more hardwares are holded as backup. This approach requires a fault detection system to monitor hardware health. When a failure is detected stand-by hardware is put into service. Boeing proposed a signal selection method using multiple redundant sensor input signals with a variable fault monitoring threshold[22] and a majority voting system[23].

In normal operation, the median value of the three air data system outputs are

used. If one of the three indications deviates too much from the other two, it is rejected by the system and the average of the remaining 2 data is accepted as true. In case the difference between these two values becomes too great, the system rejects them and autopilot disconnects. [7].

The application of majority principle might oversight failures. If 2 out-of 3 sensors are blocked and show close results, the system accepts the average of two erroneous data as accurate and eliminates the healthy one. On the other hand, hardware redundancy is vulnerable against "common mode failures"[14]. If a sensor may fail under certain conditions, it is highly probable that, all of the redundant sensors may also fail simultaneously . On November 27th, 2008 an Airbus A320 crashed with no survivors, because all of the angle of attack sensors were frozen at the same time [24]. Air France Flight 447 suffered from common mode failure as well. All of the pitot tubes on the board were blocked by ice crystals simultaneously because of the extreme cold weather. Diversity is the solution for common mode failures. Different types of sensors with different vulnerabilities should be deployed. However, airspeed could only be measured with an air data system.

Inefficacy of the hardware redundancy leads the industry towards analytical redundancy and virtual sensor concepts[25, 20].

2.2.2 Analytical Redundancy

Analytical redundancy use mathematical process models or a set of algebraic relationships to estimate reference values that are used in system health monitoring.[15, 26] Analytical redundancy applications can be classified as model-based fault diagnosis, signal-based fault diagnosis, knowledge-based fault diagnosis and hybrid fault diagnosis. Model-based fault diagnosis approaches use mathematical models of the system to estimate the sensor outputs. The difference between the measurements and the measurement estimations are taken as residuals. A reliable system model is critical for FD performance. Model uncertainties, disturbances (unknown inputs) and noise should also be considered. Residuals should be insensitive to these effects. Signal-based fault diagnosis methods, the signal

pattern and characteristics of a system operating in fault-free condition is used as reference and compared to the measured sensor signals. As the system gets complicated, mathematical models will not represent the system dynamics completely. Also there might be no explicit dynamical model of the system. Then a knowledge-based, or process history based fault diagnosis would be adequate. Large amount of historical process data is necessary. Artificial intelligence is applied to train diagnosis system that checks the sensor measurements during the operation. Although it works for complicated systems very well, unknown fault types that are not included in the training data set are hard to detect. Hybrid fault diagnosis brings together previous methods to enhance the detection capability.[27, 28]

Hansen et al. developed a fault detection algorithm for the pitot tube of a small unmanned aerial vehicle. GPS velocity measure- ments and propeller thrust readings were used to calculate airspeed with the help of the wind data taken from the ground station. These calculated airspeed data were substracted from the pitot tube output to obtain residual signals. Both raw residual signals and pre-whitened residual signals were used as detectors. Detectors gave alarms about 14 seconds after the failure [29].

Imai et al. used error signature approach to detect and accommodate pitot tube and/or GPS failure. Airspeed was calculated from GPS velocity measurement and wind data taken from the weather forecast computer. AF 447 accident scenario was studied. The failure was detected and corrected after 5 seconds from the onset of the blockage [30].

Fravolini et al. Airspeed was estimated from the flight dynamics equations. The difference between estimated airspeed and the pitot tube airspeed indication was taken as the residual. Then, the residual is whitened with an Auto Regressive (AR) process. The failure on the pitot tube was modeled as an additive offset to the airspeed. Generalized Likelihood Ratio Test was used for residual evaluation and decision making [31].

CHAPTER 3

AIR DATA SYSTEMS

3.1 Pressure Probes

Five-hole probes (5hp) are widely used in aerospace applications for flight angles and velocity calculations. A 5hp has 5 ports on the head and a static chamber on the body as shown in Figure 3.1. Flow angles are obtained from the pressure differences of the coupled pitch plane (1-3) and yaw plane ports (2-4). Dynamic pressure is found from the difference between the center port(5) and the static chamber reading (port 6).

3.2 Five-Hole Probe Calibration

The working principle of a 5hp is based on Bernoulli equation and three dimensional velocity data are extracted from pressure measurements. If the flow is uniform and 5hp is aligned with the direction of the flow, the center port mea-

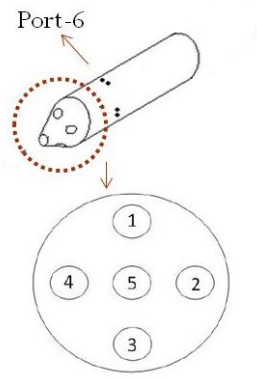

Figure 3.1: A Schematic View of a Five-Hole Probe

sures the stagnation pressure. According to Equation 3.1, airspeed is calculated directly from the dynamic pressure. However, if 5hp is not aligned with the incoming flow, dynamic pressure is built up by the velocity component in 5hp body axis direction. Hence, the orientation of the velocity vector is required to obtain total velocity from the measured dynamic pressure. This requirement is fulfilled by using the pitch and yaw plane ports pressure differences. The pitch and yaw plane pressure differences indicate angle of attack (AOA) and angle of sideslip (AOS) informations, and they are incorporated into the airspeed calculation.

$$P_t = P_s + \frac{1}{2}\rho\, V^2 \tag{3.1}$$

where P_t is stagnation pressure, P_S is static pressure, ρ is air density and V is airspeed.

It is not possible to obtain three dimensional velocity data from the measured pressures via analytical equations. Therefore, an experimental procedure is followed. A 5hp is placed in known flow fields with different AOA, AOS and Mach numbers. Then, pressure readings are recorded. It is stated that when probe pressure readings are nondimensionalized with respect to dynamic pressure, the resulting coefficients are found to be inter-related functions of AOA, AOS and Mach number [32]. Thus nondimensional coefficients are calculated from pressure data for each case. Then, a data reduction algorithm is applied with these coefficients to obtain airspeed and flow angles. This procedure is called as "5hp calibration".

Various calibration algorithms exist in the literature. Dudzinsky and Krause[33] obtained calibration coefficients using pressure difference between two ports, then used calibration maps and graphics for data reduction. Treaster and Yocum[34] defined similar coefficients and applied curve-fitting method for data reduction process. Wenger and Devenport[35] also used differential pressure readings to obtain coefficients for seven-hole pressure probe. A two-step data reduction procedure was developed. First, least squared curve fitting was applied to coefficients, and then look up table was used to correct the residual errors. Yasa and Paniagua[36] defined the coefficients for each head port. They

normalized the pressure readings with respect to the local static pressure. Since the local static pressure was one of the unknown variable, an iterative algorithm was applied with an initial static pressure estimation.

The calibration coefficients that are generally preferred are given in Equations 3.2 - 3.4.

$$C_\alpha = \frac{P_3 - P_1}{P_5 - P_6} \tag{3.2}$$

$$C_\beta = \frac{P_4 - P_2}{P_5 - P_6} \tag{3.3}$$

Gonsalez et al.[37] used a compressibility coefficient given by Equation 3.4. It is used to normalize dynamic pressure.

$$\mathbf{C}_M = \frac{P_5 - P_6}{P_5} \tag{3.4}$$

Third-order multiple regression models are used for data reduction procedure[37]. K-coefficients in Equations 3.5 - 3.7 are determined from the calibration process. Then, during the flight, pressure readings are normalized to obtain C-coefficients, and these coefficients are put in Equations 3.5 - 3.7 to calculate AOA, AOS and airspeed.

$$\alpha = K_{0,\alpha} + K_{1,\alpha}C_\alpha + K_{2,\alpha}C_\beta + K_{3,\alpha}C_M + .. + K_{19,\alpha}C_\alpha C_\beta C_M \tag{3.5}$$

$$\beta = K_{0,\beta} + K_{1,\beta}C_\alpha + K_{2,\beta}C_\beta + K_{3,\beta}C_M + .. + K_{19,\beta}C_\alpha C_\beta C_M \tag{3.6}$$

$$M = K_{0,M} + K_{1,M}C_\alpha + K_{2,M}C_\beta + .. + K_{19,M}C_\alpha C_\beta C_M \tag{3.7}$$

3.3 The New Calibration Algorithm

Small particles, insects, debris may easily block probe ports. Even if one port is blocked, current approaches fail to give correct data. Because, the calibration coefficients in Equations 3.2 - 3.4 do not allow to isolate an erroneous measurement from the rest of the calculations. As a solution, redundant coefficients are proposed for each air data parameter[38]. AOA estimation primarily depends on ports 1 and 3, whereas for AOS, ports 2 and 4, and for airspeed calculation port 5 are more critical. It is aimed to estimate AOA, AOS and airspeed correctly even if one of their critical ports is blocked. Therefore, new coefficients are defined for each critical port as given in Equations 3.8

$$C_1 = \frac{P_1 - P_6}{P_5 - P_6} \quad C_2 = \frac{P_2 - P_6}{P_5 - P_6}$$

$$C_3 = \frac{P_3 - P_6}{P_5 - P_6} \quad C_4 = \frac{P_4 - P_6}{P_5 - P_6} \tag{3.8}$$

$$C_{av} = \frac{P_{av} - P_6}{P_6}$$

An example of the differences between traditional and new approaches are shown schematically in Figure 3.2 - Figure 3.3. When port 1 is blocked, traditional methods give incorrect C_α coefficient and this leads to wrong AOA calculation. On the other hand, it is still possible to obtain correct result with the new algorithm. It continues with the redundant coefficient C_3 to find AOA. Therefore it becomes possible to keep using 5hp when any port is blocked.

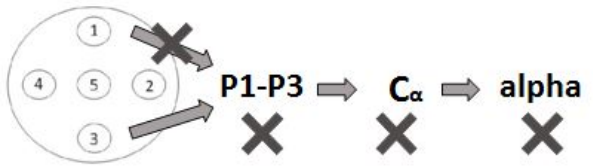

Figure 3.2: Traditional Calibration Approaches

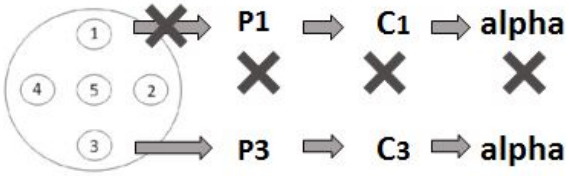

Figure 3.3: The New Calibration Approach

Table 3.1 gives the coefficients that will be used for AOA, AOS and Mach number calculations in case any head port is blocked.

Table3.1: Calibration Coefficient Selection for Different Scenarios

	AOA	AOS	Airspeed
No blockage	C_1&C_3	C_2&C_4	C_M
Blocked port: 1	C_3	C_2&C_4	C_M
Blocked port: 2	C_1&C_3	C_4	C_M
Blocked port: 3	C_1	C_2&C_4	C_M
Blocked port: 4	C_1&C_3	C_2	C_M
Blocked port: 5	C_1&C_3	C_2&C_4	C_{av}

If there is no blockage Equations 3.9- 3.11 are used. If, as an example, port 1 is blocked, faulty pressure reading is isolated from the calculations by using C_3 instead of C with Equations 3.12- 3.14.

$$\alpha = K_{0,\alpha}+K_{1,\alpha}(C_1-C_3)+K_{2,\alpha}(C_4-C_2)+K_{3,\alpha}C_M+..+K_{19,\alpha}(C_1-C_3)(C_4-C_2)C_M \tag{3.9}$$

$$\beta = K_{0,\beta}+K_{1,\beta}(C_1-C_3)+K_{2,\beta}(C_4-C_2)+K_{3,\beta}C_M+..+K_{19,\beta}(C_1-C_3)(C_4-C_2)C_M \tag{3.10}$$

$$M = K_{0,M} + K_{1,M}(C_1 - C_3) + K_{2,M}(C_4 - C_2) + .. + K_{19,M}(C_1 - C_3)(C_4 - C_2)C_M \tag{3.11}$$

$$\alpha = Ka_{0,1} + Ka_{1,1}C_3 + Ka_{2,1}(C_4 - C_2) + Ka_{1,1}C_M + .. + Ka_{19,1}C_3(C_4 - C_2)C_M \tag{3.12}$$

$$\beta = Kb_{0,1} + Kb_{1,1}C_3 + Kb_{2,1}(C_4 - C_2) + .. + Kb_{19,1}C_3(C_4 - C_2)C_M \tag{3.13}$$

$$M = Km_{0,1} + Km_{1,1}C_3 + Km_{2,1}(C_4 - C_2) + .. + Km_{19,1}C_3(C_4 - C_2)C_M \tag{3.14}$$

It is necessary to have a unique relationship between coefficients and angles, so that only one solution set exists for air data. Hence, the coefficient trends are critical and should be observed. Wind tunnel test results were used to obtain calibration coefficients. Both the traditional and new approaches were examined for comparison. Figure 3.4 shows the contour plots of coefficients with respect to AOA and beta.

Plot (a) and (d) show AOA and AOS coefficients found from traditional way with Equation 3.2 - 3.3. Plot (b), (c), (e) and (f) show port coefficients calculated from Equation 3.8. It is shown that the coefficient contours do not intersect each other both for the traditional and the new approaches. Each alpha and beta combination is represented by a unique value.Therefore uniqueness of solution is satisfied. Thus it is deduced that the new coefficients might substitute the traditional ones.

Different port blockage scenarios given in Table 3.1 were studied for all the test points. When a port is blocked, it is identified by the fault detection algorithm proposed in Chapter 5 and data reduction is conducted with redundant coefficient.

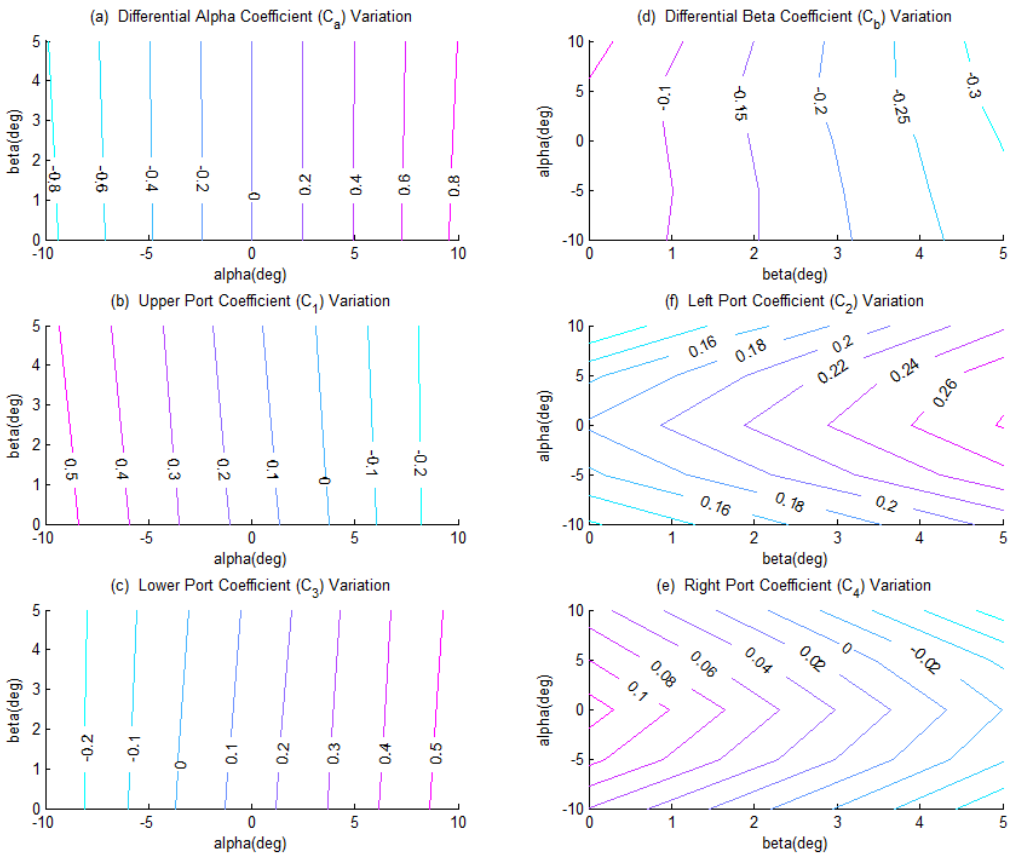

Figure 3.4: Comparison of Calibration Coefficients

Table3.2: Goodness of Fit For Estimations

	alpha		beta		Mach	
	NRMSE	RMSE	NRMSE	RMSE	NRMSE	RMSE
No blockage	0.9962	0.1662	0.9970	0.0879	0.9936	0.0179
Port-1 is blocked	0.9930	0.2245	0.9969	0.0885	0.9936	0.0179
Port-2 is blocked	0.9949	0.1917	0.9788	0.2320	0.9957	0.0146
Port-3 is blocked	0.9949	0.1919	0.9970	0.0871	0.9935	0.0180
Port-4 is blocked	0.9959	0.1715	0.9851	0.1948	0.9957	0.0147
Port-5 is blocked	0.9927	0.2296	0.9845	0.1984	0.9831	0.0290

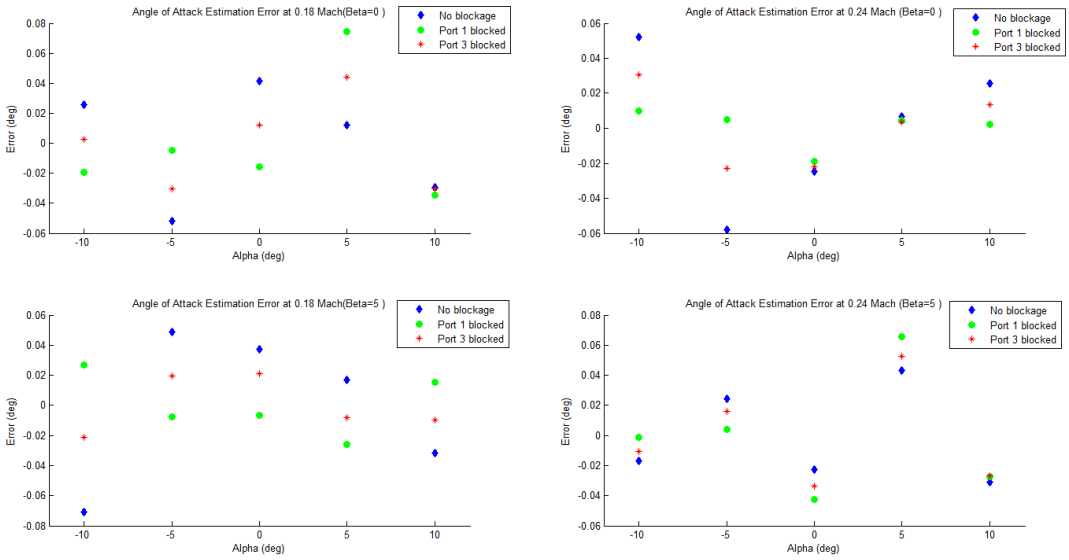

Figure 3.5: Alpha Estimation Error

Table 3.2 shows the goodness of fit in terms of Normalized Root Mean Square Error(NRMSE) and Root Mean Square Error(RMSE) for AOA, AOS and airspeed estimation for 6 scenarios. It can be observed that even a critical port is blocked errors are small and close to the no-blockage scenario results.

Figure 3.5- 3.6 shows the obtained error at each test point for different Mach numbers. It is observed that although one port is blocked results are still reliable. Mach number and velocity errors are given in Figure 3.7. Even though the center port is blocked airspeed estimation accuracy is still high.

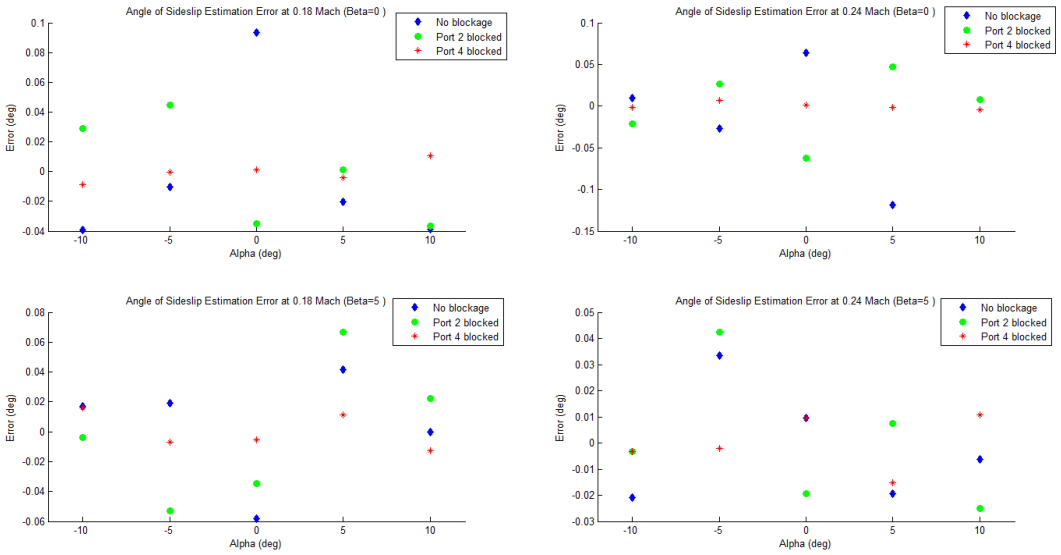

Figure 3.6: Beta Estimation Error

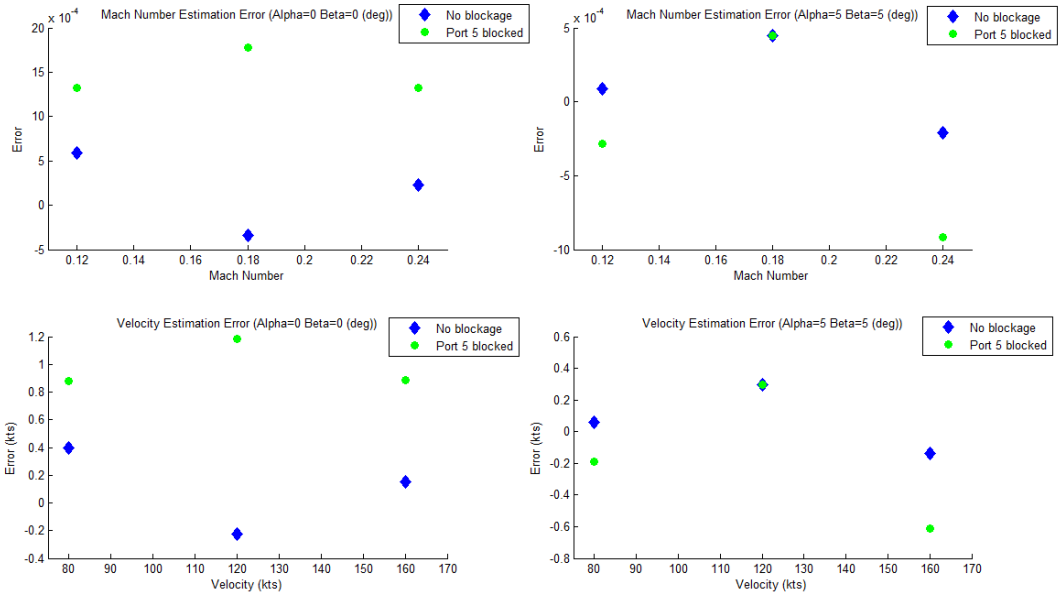

Figure 3.7: Mach Estimation Error

CHAPTER 4

PROBLEM FORMULATION

It is important to understand the characteristics of fault to design an appropriate fault detection algorithm that satisfies the performance criteria mentioned in Chapter 2.

Air France 447 (AF 447) accident report [7] provides a comprehensive analysis. Flight Data Recorders (FDR) and Cocpit Voice Recorders (CVR) recovered from the wreckage provided important data to understand the mechanism and results of pitot tube icing. According to the report, the aircraft took off at 22:30 on June 1,2009 and crashed into the Atlantic Ocean at around 02:15. The causes of the accident lies within the last five minutes of the flight, when the pitot tubes obstructed by ice crystals. Until that moment, flight continued safely without any problem. Details of the accident and flight history are investigated through this chapter.

4.1 Consequences of a Blocked Port on Measurements

Pressure ports are faced towards the incoming flow and total pressure, which is the sum of the dynamic and static pressure is measured within these ports.

If the inlet of a port is blocked totally, pressure trapped inside the port equals to the static pressure at the time of obstruction. Pressure sensed from this port is equal to that trapped pressure and remains constant throughout the blockage. Airspeed is calculated from the difference between the total and static pressures. Therefore, if the center port is blocked before the take-off, indicated

airspeed shows zero throughout the runway pass. As the altitude increases, static pressure decreases, whereas the total pressure reading remains constant due to the blockage. Thus as aircraft climbs, this difference grows continuously, and airspeed is indicated higher than the actual value. Actually, this was the case for Birgenair Flight Accident [4, 5]. On the other hand, airspeed failure showed a different trend for AF 447. It suffered from a sudden decrease in airspeed. The reason was, aircraft was in the cruise phase when the blockage happened, and stayed around that level. Static pressure did not decrease dramatically, but the measured total pressure drops suddenly after the obstruction, and consequently indicated airspeed decreased.

Figure 4.1 [7] shows the effect of obstruction on total pressure, pressure altitude and baro-inertial vertical speed for Air France 447 flight. Airbus 330 has 3 pitot-tubes. ADR 1 is Captain pitot tube, ADR 2 is First Officer pitot tube and ADR 3 is Standby pitot tube.

Figure 4.1 shows the result of a wind tunnel test conducted with a blocked and healthy pitot tubes. Blockage is at the center port, Port 5. Output of the healthy pitot tube is given as reference total pressure. It is observed that pressure trapped inside the blocked port is equal to static pressure and stays constant.

4.2 Air France 447 Accident Analysis

Figure 4.2 shows the flight data displayed on the left PFD and ISIS. A sharp decrease in computed airspeed is observed at 02:10:07. It is estimated that both pitot tubes were frozen at that time. For the right pitot tube, it is thought that it started to freeze at the earliest at 2 h 10 min 03.5 and at the latest at 2 h 10 min 05. The CAS (Calibrated Air Speed) 2 was then more or less equal to CAS 1 and thus equal to the airspeed recorded by the FDR. Icing history for three pitot tubes are given in Figure 4.4 .

Flight control primary computers (PRIM) monitor and validate air data they use. A voting mechanism is applied among 3 pitot tube outputs. If one of

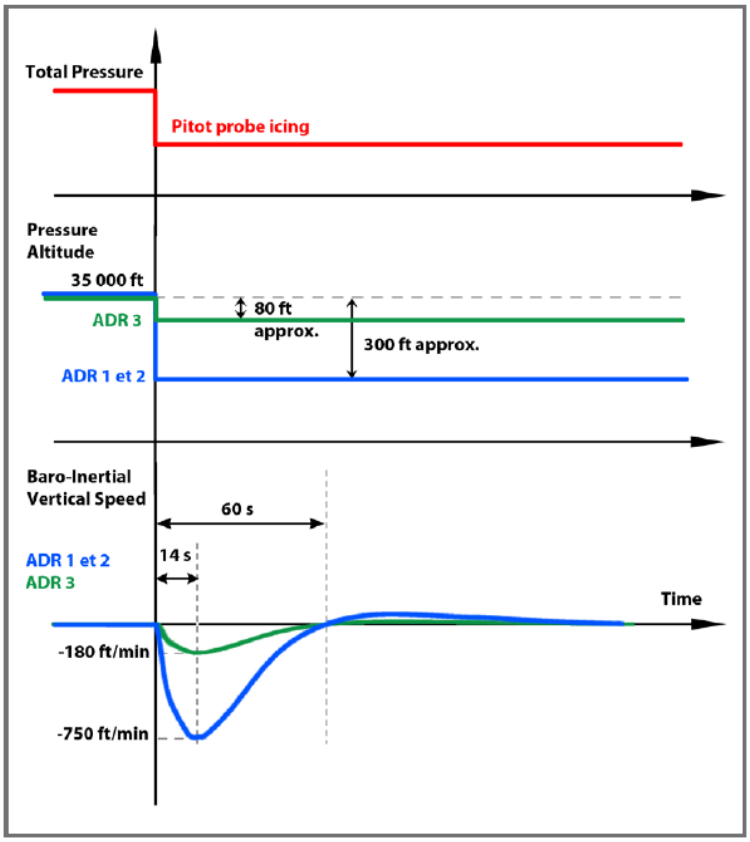

Figure 4.1: Effect of a drop in total measured pressure on pressure altitude and vertical speed -BEA, "Final Report: On the accident on 1st June 2009 to the Airbus A330-203 registered F-GZCP operated by Air France flight AF 447 Rio de Janeiro - Paris",2012

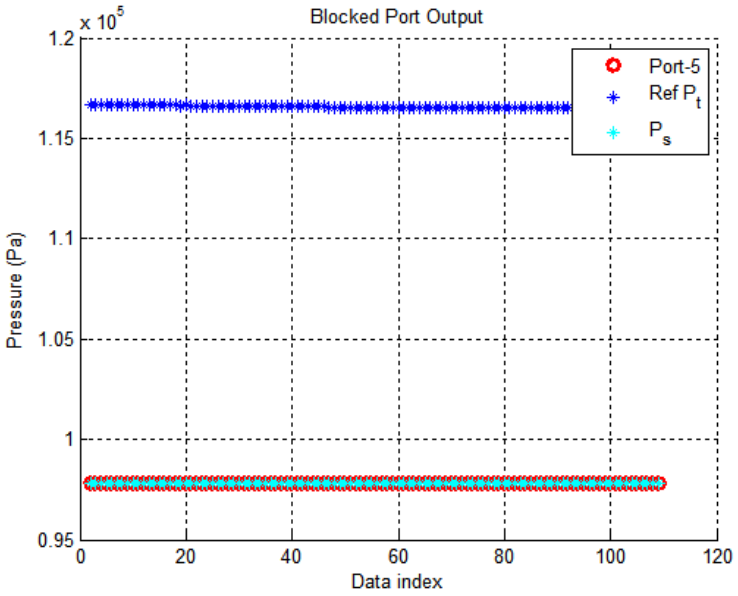

Figure 4.2: Wind Tunnel Test of a blocked port

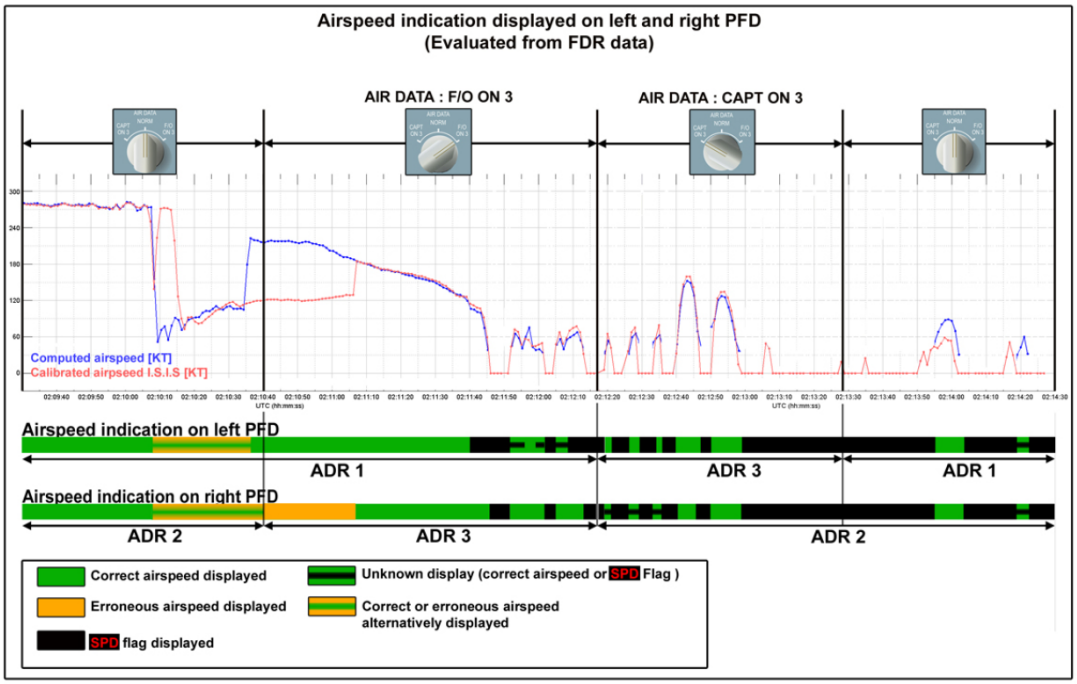

Figure 4.3: Speed displays on the Primary Flight Display (PFD)-BEA, "Final Report: On the accident on 1st June 2009 to the Airbus A330-203 registered F-GZCP operated by Air France flight AF 447 Rio de Janeiro - Paris",2012

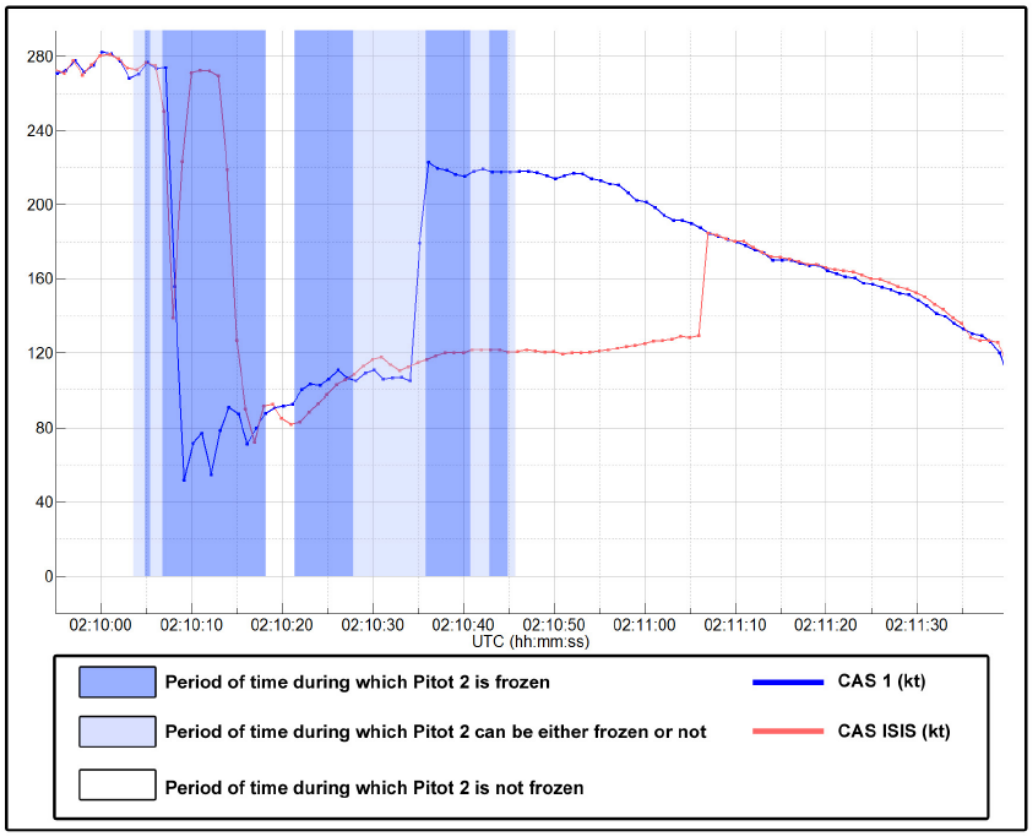

Figure 4.4: Pitot Tube Frozen Period-BEA, "Final Report: On the accident on 1st June 2009 to the Airbus A330-203 registered F-GZCP operated by Air France flight AF 447 Rio de Janeiro - Paris",2012

the airspeeds deviates too much from the others, it is rejected by the computer and the average of the other two are taken as voted airspeed and displayed on PFD. If the difference between these 2 airspeed increases, then these airspeeds are rejected too, and flight mode changes to Alternate 2 and no speed data is displayed on PFD. On the other hand, voted airspeed is always monitored, when it falls by more than 30 kt. in one second, it is rejected as well and Alternate 2 mode is triggered. Within the framework of this algorithm, when 2 pitot tubes frozen and outputs close results to each other, it is possible that erroneous airspeed will be displayed and used in the altitude and temperature corrections.

From the flight data chronology, Figure 4.5 , it is seen that after the autopilot disconnection, altitude indication decreased 360 ft. in 4 seconds. However true altitude did not change that much. This erroneous display caused by incorrect

airspeed data used in altitude corrections. As a reaction this change, pilot made a pitch up maneuver. Investigators estimated the true Mach number from the ground speed, wind and static temperature. Figure 4.6, shows the comparison of true and displayed Mach numbers. As a result of pilot commands, aircraft stalled and crashed into the ocean.

Figure 4.7- 4.8 shows wind and turbulence condition that the aircraft was exposed to.

In Appendix A, Figure .1- .2- .3 show the flight history and cocpit voice recordings. Figure .4 shows the last 5 minutes of the flight.

4.3 Findings

The following remarks are made based on the accident analysis and port blockage studies.

- Fault detection algorithm should be fast. Early detection and rejection will prevent usage of erroneous data in consequent altitude, vertical speed and temperature corrections.
- Consequences of a blocked port on air data parameters depend on at which flight phase it occurs. If it happens before the flight, total pressure measured will be constant and equal to the static pressure at the ground level. If it happens during a cruise, measured pressure will abruptly decrease from total pressure to the static pressure at that level. In the scope of this thesis, cruise-level blockages were studied.
- When a port is obstructed at cruise, measured pressure is around static pressure and stays almost constant. Only small fluctuations due to pressure transducer noise are expected. Therefore, a sudden drop in signal energy is observed.
- Instead of constant wind assumption, time-varying wind with turbulence should be studied to make the scenarios more realistic.

- When the airspeed error is detected, speed display goes off and autopilot disconnects. All of a sudden, flight crew find themselves controlling the aircraft without a valid flight data. Most of the time, they were not aware of the real problem. Therefore, fault accommodation is very critical.

UTC Time	Altitude (ft), ISIS Altitude (ft)	FDR Parameters
2 h 10 min 05	35,024	The A/P2 disconnects.The roll angle changes from 0 to 8.4° in 2 seconds whereas the sidestick is at neutral. The pitch attitude is 0°.
2 h 10 min 08		The FD 1 and 2 become unavailable. The CAS changes from 274 kt to 156 kt. The CAS ISIS changes from 275 kt to 139 kt then goes back up to 223 kt. The Mach changes from 0.80 to 0.26.
2 h 10 min 09	34,664 34,900	The CAS is 52 kt. The CAS ISIS stabilises at 270 kt for 4 seconds.
2 h 10 min 10		The stall warning is triggered.
2 h 10 min 12		The CAS ISIS changes from 270 kt to 73 kt in 4 seconds while the CAS is 55 kt.
2 h 10 min 17	34,976	The FD 1 and 2 become available again. The CAS is 80 kt and the CAS ISIS is 92 kt.
2 h 10 min 21		The FD 1 and 2 become unavailable. The CAS is 93 kt and the CAS ISIS is 83 kt. The Mach is 0.29.
2 h 10 min 26		The FD 1 and 2 become available again
2 h 10 min 34		The CAS increases from 105 kt to 223 kt in 2 seconds. The CAS ISIS is 115 kt.
2 h 10 min 36	37,124	The FD 1 and 2 are unavailable
2 h 10 min 39 → 2 h 10 min 46		The 'AIR DATA' selector then the 'ATT/HDG' selector are positioned on "F/O on 3".
2 h 10 min 42		The FD 1 and 2 become transiently available (HDG/VS modes). The selected heading is 36°. The vertical speed is 1,900 ft/min and the vertical speed selected is 1,300 ft/min.
2 h 10 min 47		The FD 1 and 2 become available again (modes HDG/ VS).

Figure 4.5: AF 447 Flight Data Recorder Chronology-BEA, "Final Report: On the accident on 1st June 2009 to the Airbus A330-203 registered F-GZCP operated by Air France flight AF 447 Rio de Janeiro - Paris",2012

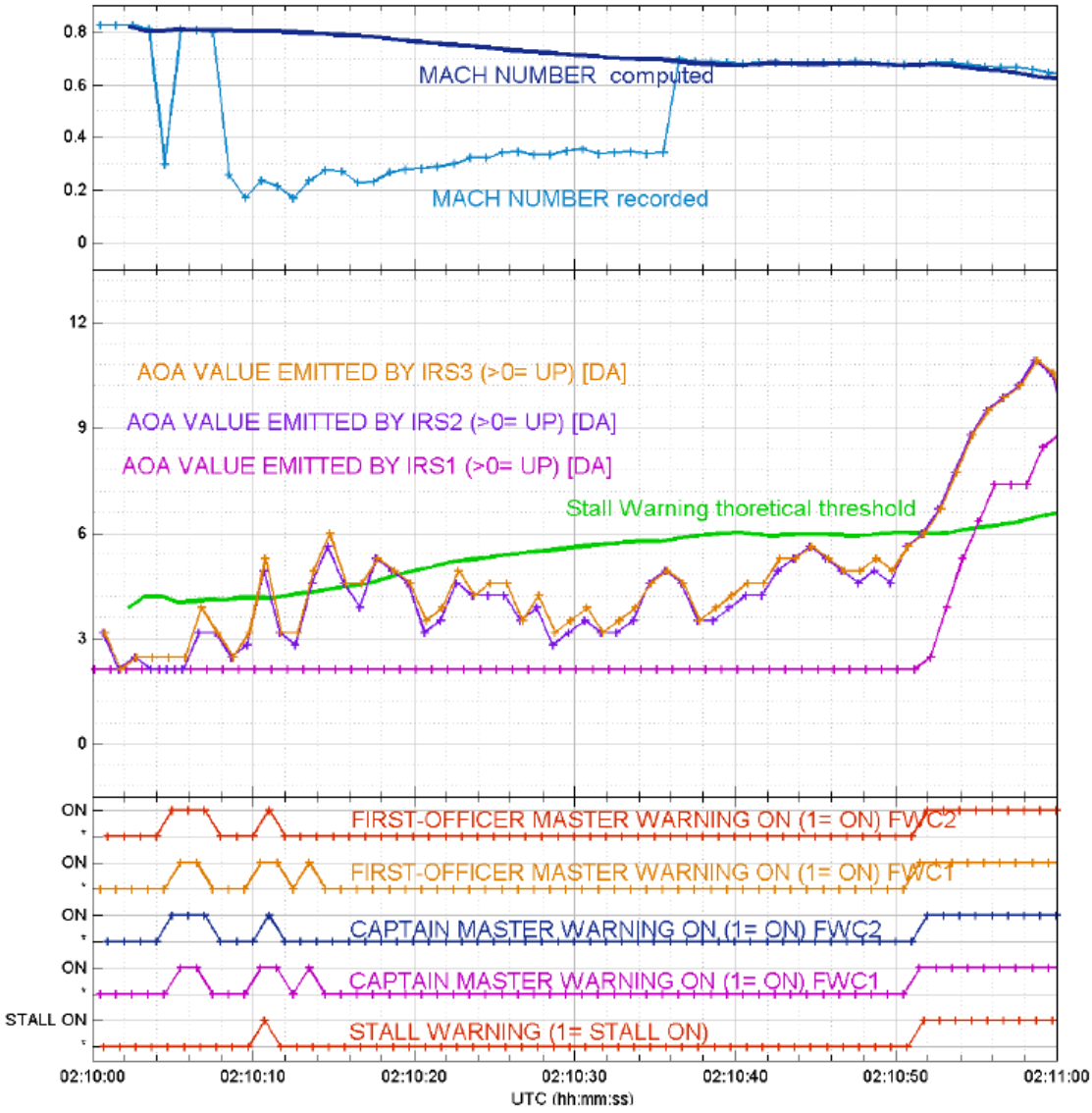

Figure 4.6: Evolutions of recorded angles of attack and of the stall warning trigger threshold-BEA, "Final Report: On the accident on 1st June 2009 to the Airbus A330-203 registered F-GZCP operated by Air France flight AF 447 Rio de Janeiro - Paris",2012

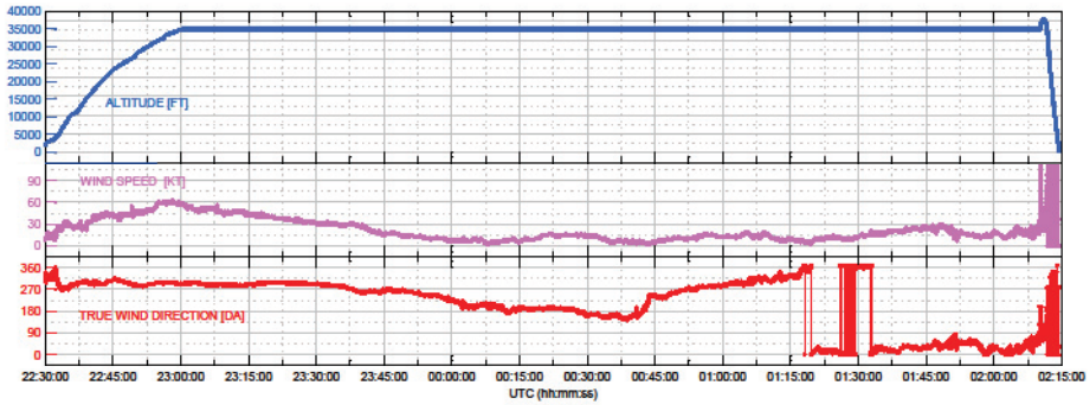

Figure 4.7: Wind velocity and direction-BEA, "Final Report: On the accident on 1st June 2009 to the Airbus A330-203 registered F-GZCP operated by Air France flight AF 447 Rio de Janeiro - Paris",2012

Start	End	Duration	Amplitude
22:30	23:45	1h15	<=0,2
23:45	1:02	1h17	calm
1:02	1:32	30 min	<=0,15
1:32	1:36	4 min	0,2
1:36	1:45	9 min	<=0,1
1:45	1:48	3 min	0,2
1:48	1:52	4 min	0,3 – 0,4
1:52	2:02	10 min	<=0,15
2:02	2:07	5 min	increase from 0,1 to 0,25
2:07	2:10	3 min	maximum 0,5

Figure 4.8: Level of turbulence during the flight-BEA, "Final Report: On the accident on 1st June 2009 to the Airbus A330-203 registered F-GZCP operated by Air France flight AF 447 Rio de Janeiro - Paris",2012

CHAPTER 5

METHODOLOGY

In the light of the findings of Chapter 4 an air data system fault detection and accommodation algorithm was designed. A 6 DOF Simulink model was used to design and test the algorithm.

5.1 Simulation

A 6 DOF Boeing 747 model was used to simulate aircraft cruise level dynamics. Wind and turbulence models are introduced. Wind is given in 3 direction. Turbulence model is taken from Matlab/Simulink library, Dryden Wind Turbulence Model. Five-hole probe wind tunnel results are embedded as lookup tables to model the pressures built at each port. 6 lookup tables used for 5 ports on the head and 1 static chamber. Lookup table dimensions are given as angle of attack (AOA), angle of sideslip(AOS) and airspeed in Mach number(M). AOA,AOS and airspeed outputs of 6 DOF Boeing model is fed into the five-hole probe model. Corresponding pressures are taken from lookup tables and sent to health monitoring system. This system monitors output pressures and generate *healthy flag* or *fault flag* that indicate health status for each port. Monitoring system sends port pressures and flags to air data computing algorithm. This algorithm uses five-hole probe calibration equations to calculate AOA, AOS and airspeed. Air data outputs of the algorithm are fed into a data fusion system. This system checks the health condition of each port and determine whether to use or not the outputs of five-hole probe sensor. INS and GPS measurements are also input to the data fusion system. Using the kinematic relations air data

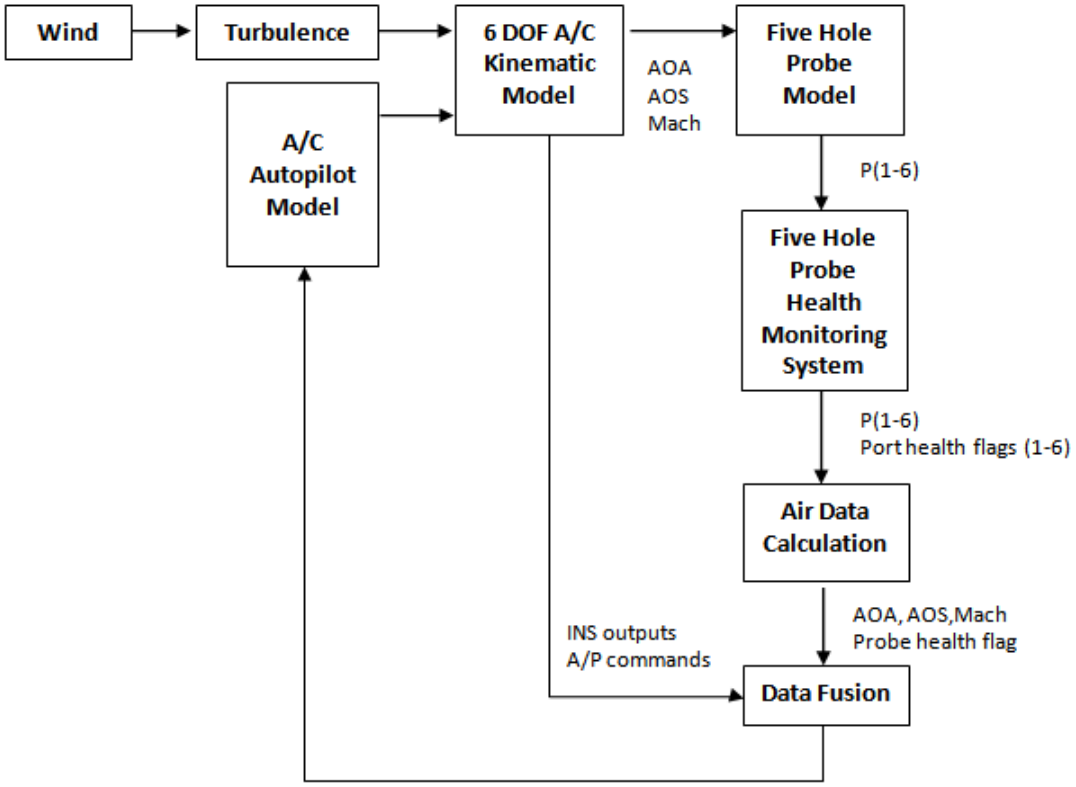

Figure 5.1: Outline of the Simulation

are estimated. The outline of the simulation is given in Figure 5.1. Simulation runs at 100Hz, whereas five-hole probe model at 50 Hz and aircraft model at 20 Hz.

5.2 Fault Detection Method

5.2.1 Residual Generation

A residual is used to monitor system health[11]. Performance criteria mentioned in Chapter 2 should be considered for residual selection. It should be sensitive to failures and insensitive to any disturbance. Various methods, such as model based and signal based, exist in the literature for residual generation. It depends

on the failure mechanism and sensor characteristics to select an appropriate residual.

Model based methods generate reference air data values from kinematic or dynamic equations. Then the difference between Air Data System outputs and reference values are taken as residuals. Generally, constant wind assumption is used in model based fault detection methods. Stochastic processes such as turbulence and time varying wind speed are problems in model based fault detections. It may cause false alarms and unreliable monitoring systems. For some applications, wind data are taken from the weather forecast computer [30], however this introduce a hardware dependency to the FDA algorithm.

On the other hand, considering the behavior of an obstructed port measurement, signal based approach promises a better solution for abrupt air data system failures. Energy level of pressure signal is suddenly decreases and stays at that level throughout the blockage. Monitoring the pressure signal, it is possible to detect abrupt changes that corresponds to port obstruction. Frequency level differences between wind, aircraft dynamics and obstruction will be used to obtain an appropriate monitoring signal that gives maximum reaction to blockage caused pressure changes and minimum reaction to disturbance related pressure changes.

First order difference equation was used for online filtering of pressure data and to remove the effects of wind and aircraft dynamics that have lower frequency compared to blockage effect. Different time window size were chosen, i.e [0.5-1-2-3-5] seconds. Backward difference was taken for each data for all window size. Difference formula is given in Equation 5.1, where w corresponds to window size. Filtered data were used as monitoring residual signals. It is desired to have minimum reaction to disturbances and fast response to failure. Different disturbances were studied to observe the trend of filtered signal at various time window size, and then determine the appropriate one. Results are given in Figure 5.2- 5.6.

$$P_w(t)) = P(t) - P(t-w) \tag{5.1}$$

5.2.2 Adaptive Threshold Setting

Threshold for fault alarm will set online adaptively considering residual data. Window shifted mean and standard deviation of residual signal are obtained. Data sampling frequency is 100 Hz. and window size is selected as 0.1 sec. In the simulation, first 1000 samples of pressure data are used to initialize threshold limits. Therefore, no fault detection is conducted meanwhile. Standard deviation is multiplied with 5 and 10 for trial , then added to mean value to create the upper and lower limits of monitoring system, as given in Equation 5.2. Time varying wind with light, moderate and severe turbulence scenarios are studied to the threshold limit and determine the gain to multiply standard deviation. Figure 5.7- 5.13 show the results. Considering the high turbulence level, it is safer to select the gain higher or equal to 10. Threshold setting is very critical. As described in Chapter 2, it should be large enough to avoid false alarms due to disturbances etc, and small enough to not to miss any failure and be fast.

$$P_{thr(t)} = \bar{P(t)} \pm \gamma\sigma(t) \tag{5.2}$$

where $\bar{P(t)}$ and $\sigma(t)$ correspond to window shifted mean and standard deviation of monitored pressure data. γ is a pre-determined threshold gain. Pressure levels are different for each port, so it should be a adjusted according to selected port.

Wind and altitude change are 2 prominent factors that effect measured pressure. Therefore time variant wind, turbulence and changing altitude scenarios were studied. Details of the scenarios are given in Table 5.1. First 3 case were studied for residual selection and the last case studied for threshold determination. Simulation results are given in Figure 5.2 - 5.13. Small window size eliminates environmental disturbances. As the window size increases effect of low frequency components become significant. Residual signal should be close to 0 as much as possible when there is no failure to decrease the threshold limit. Window size 0.5 sec. arises as the most suitable one for fault monitoring in all cases.

Table5.1: Fault Detection Case Study Scenarios

Case	Altitude change (m/s)	Wind velocity change	Turbulence
1	Constant altitude	Time varying wind	No
1.1		Amp: 5m/s Freq:0.02 rad/s	
1.2		Amp: 15m/s Freq:0.01 rad/s	
1.3		Amp: 15m/s Freq:0.03 rad/s	
2	Constant altitude	Constant wind	Yes
2.1		[10 10 -5]	10^{-2} - Light
2.2		[10 10 -5]	10^{-3} - Moderate
2.3		[10 10 -5]	10^{-5} - Severe
3	Altitude Change	Constant wind	No
3.1	5 m/s for 60 sec.	[10 10 -5]	
3.2	10 m/s for 60 sec.	[10 10 -5]	
3.3	20 m/s for 60 sec.	[10 10 -5]	
3.4	50 m/s for 60 sec.	[10 10 -5]	
4	Constant altitude	Time varying wind	Yes
4.1		Amp: 15m/s Freq:0.02 rad/s	10^{-2} - Light
4.2		Amp:1 5m/s Freq:0.02 rad/s	10^{-3} - Moderate
4.3		Amp: 15m/s Freq:0.02 rad/s	10^{-5} - Severe
4.4		Amp: 30m/s Freq:0.02 rad/s	10^{-2} - Light
4.5		Amp: 30m/s Freq:0.02 rad/s	10^{-3} - Moderate
4.6		Amp: 30m/s Freq:0.02 rad/s	10^{-5} - Severe

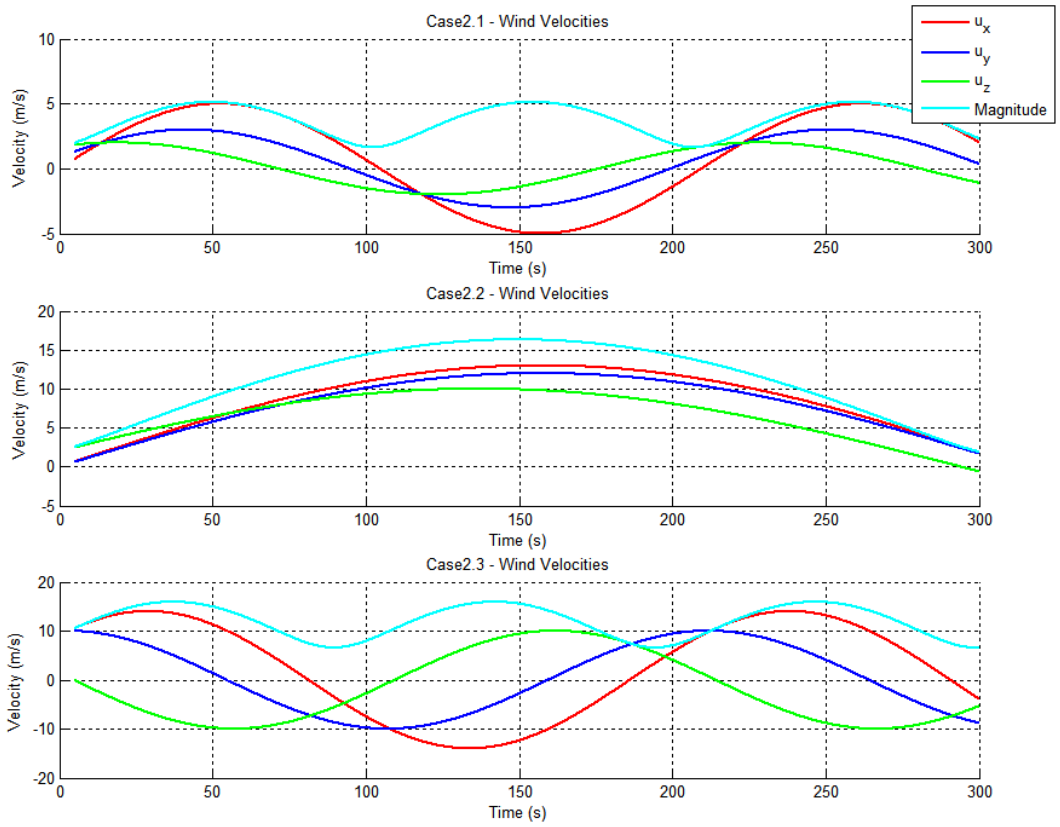

Figure 5.2: Case1: Wind Data

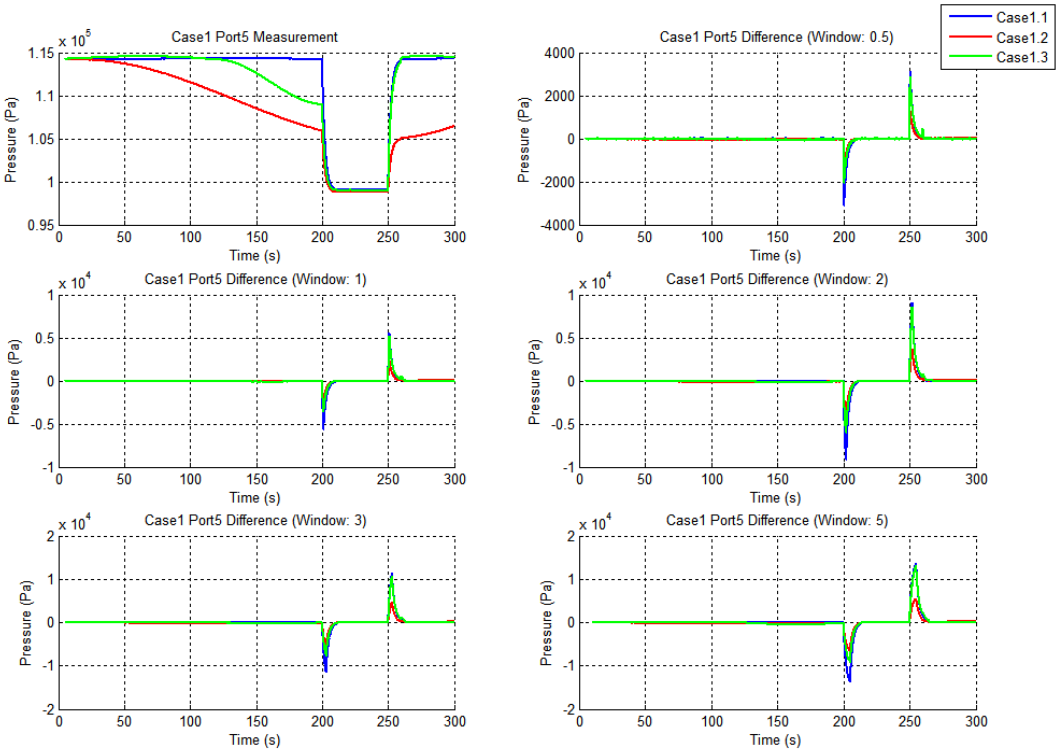

Figure 5.3: Case1: Port 5 pressure change and time-windowed results

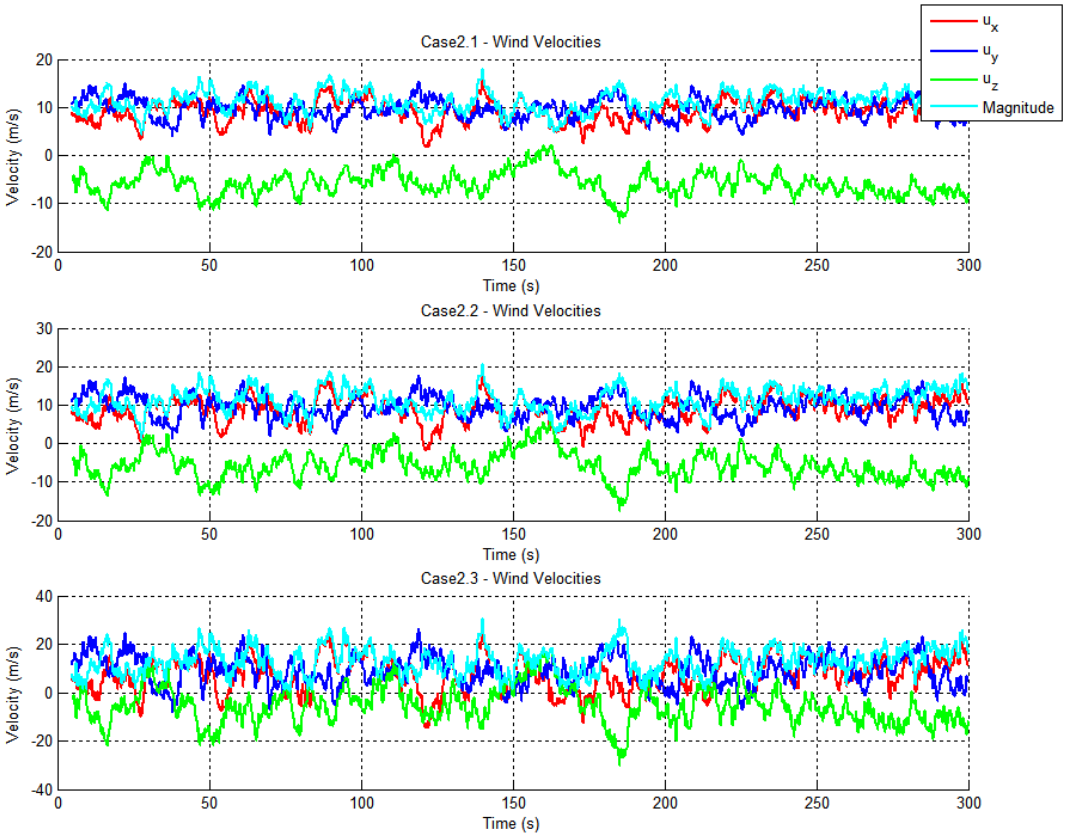

Figure 5.4: Case2: Wind Data

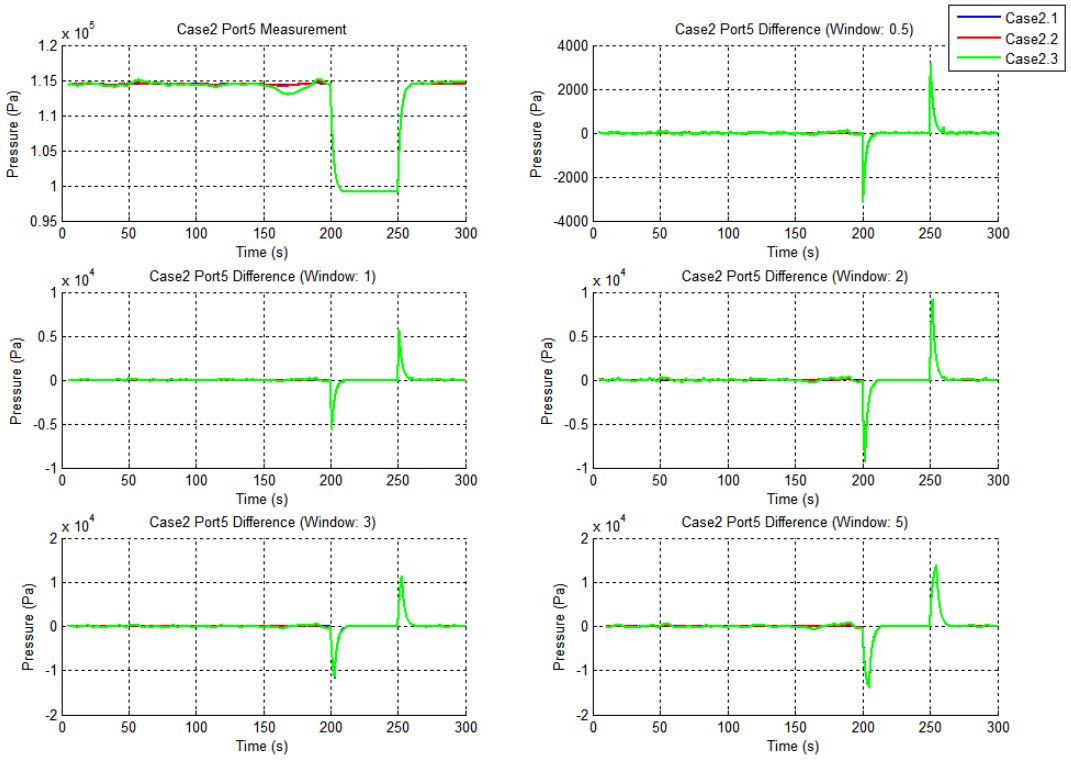

Figure 5.5: Case2: Port 5 pressure change and time-windowed results

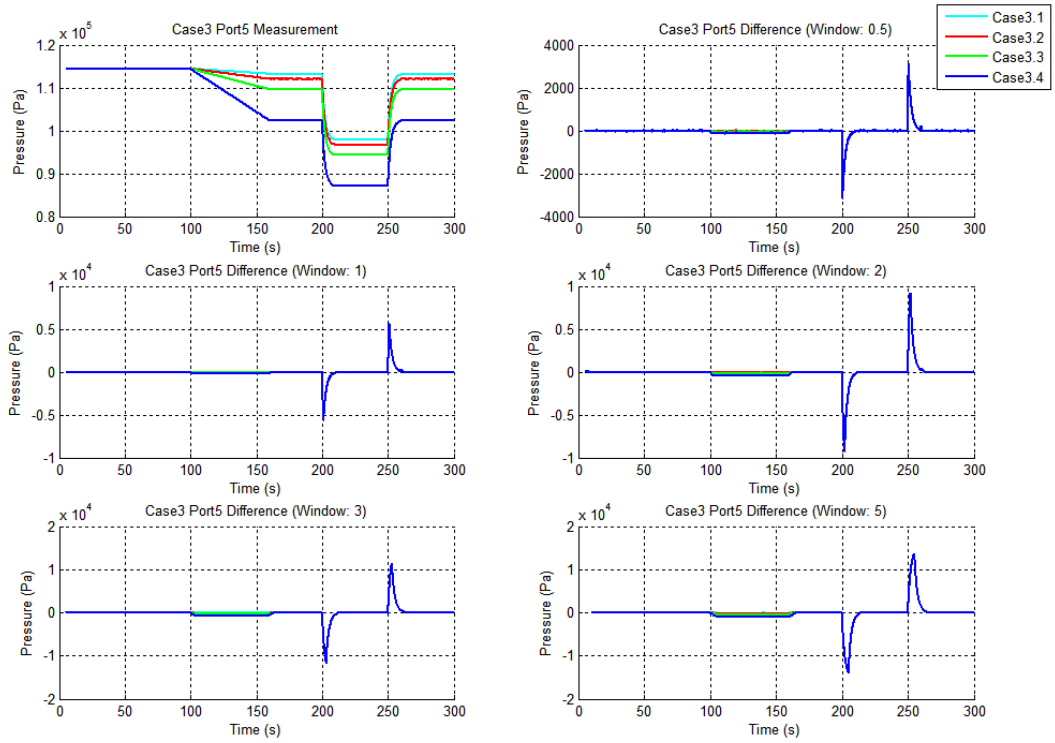

Figure 5.6: Case3: Port 5 pressure change and time-windowed results

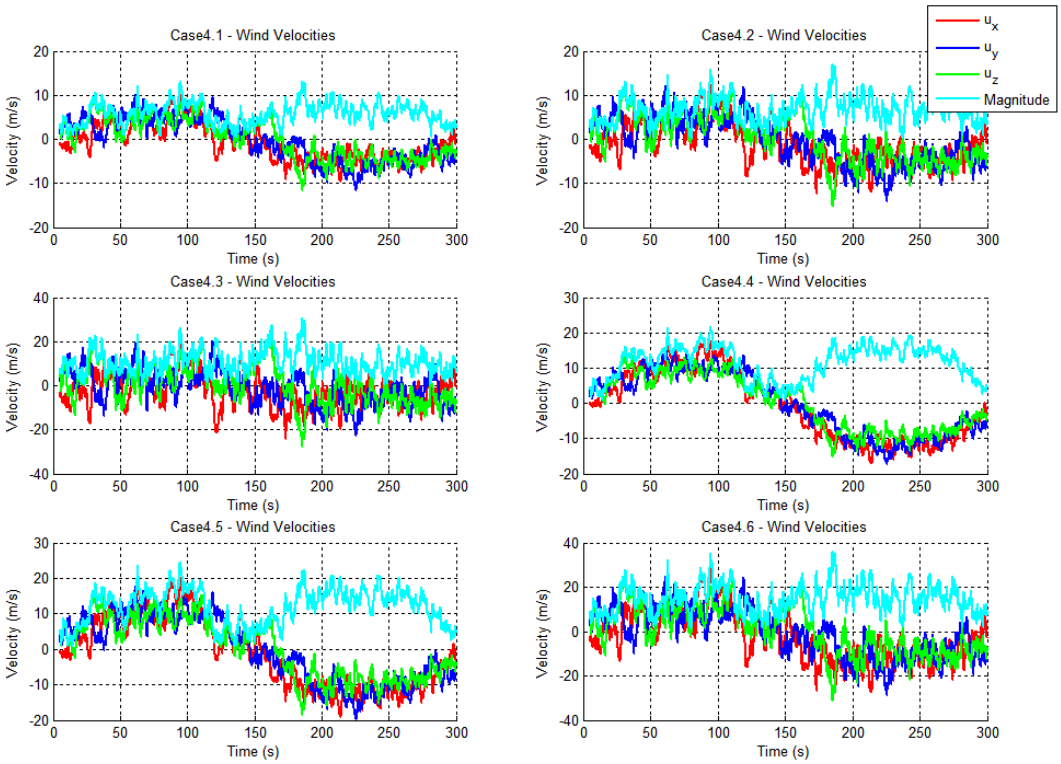

Figure 5.7: Case4: Wind Velocities

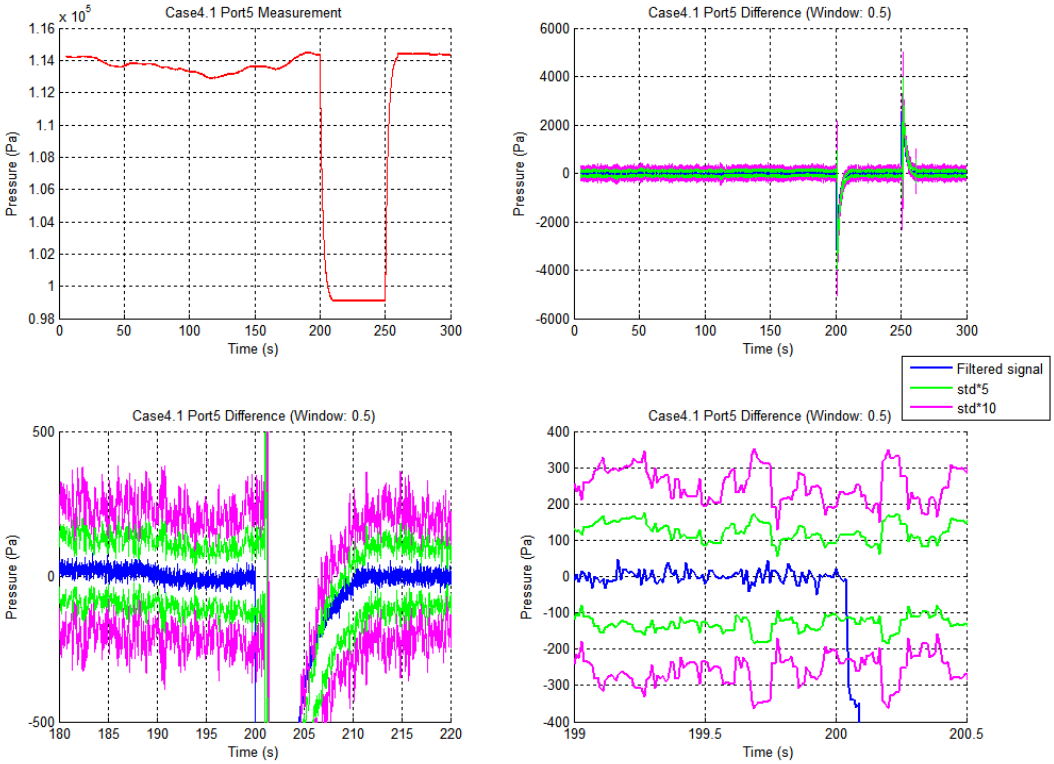

Figure 5.8: Case4.1: Thresholds and Fault Detection

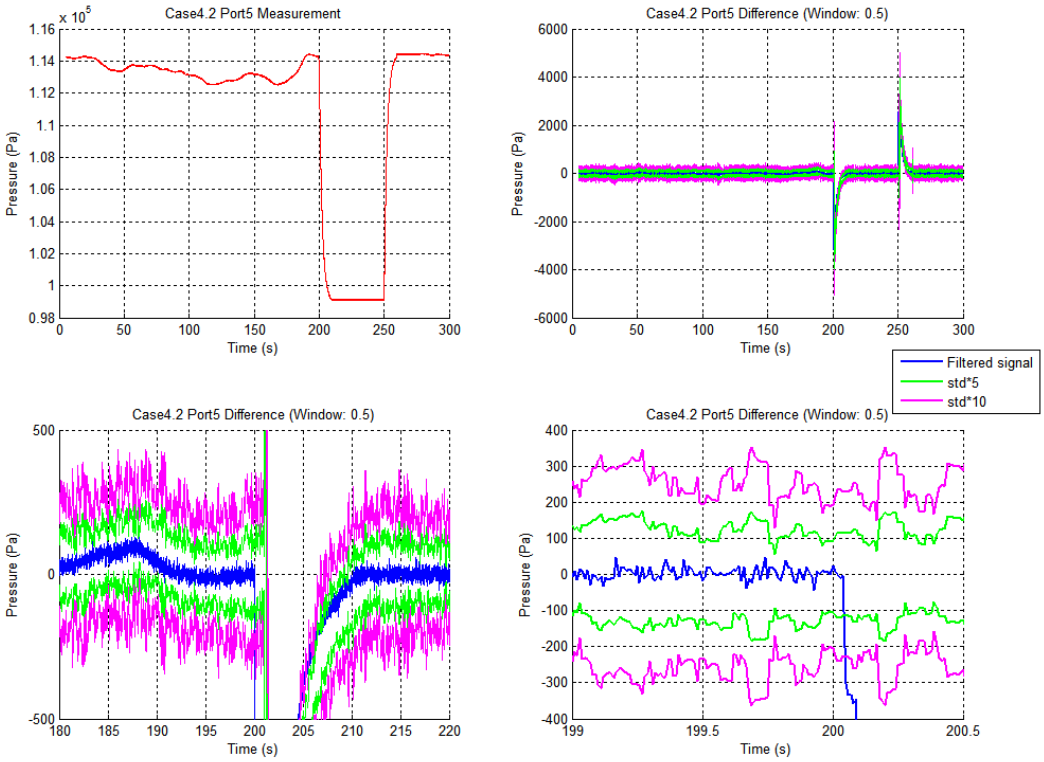

Figure 5.9: Case4.2: Thresholds and Fault Detection

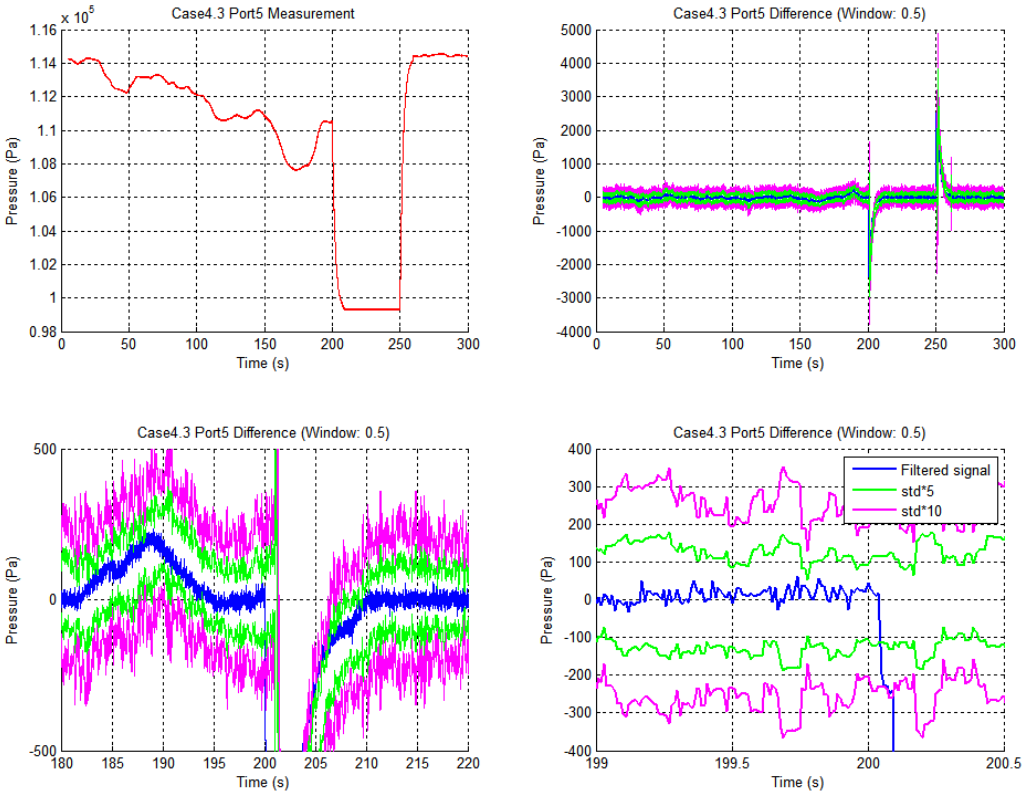

Figure 5.10: Case4.3: Thresholds and Fault Detection

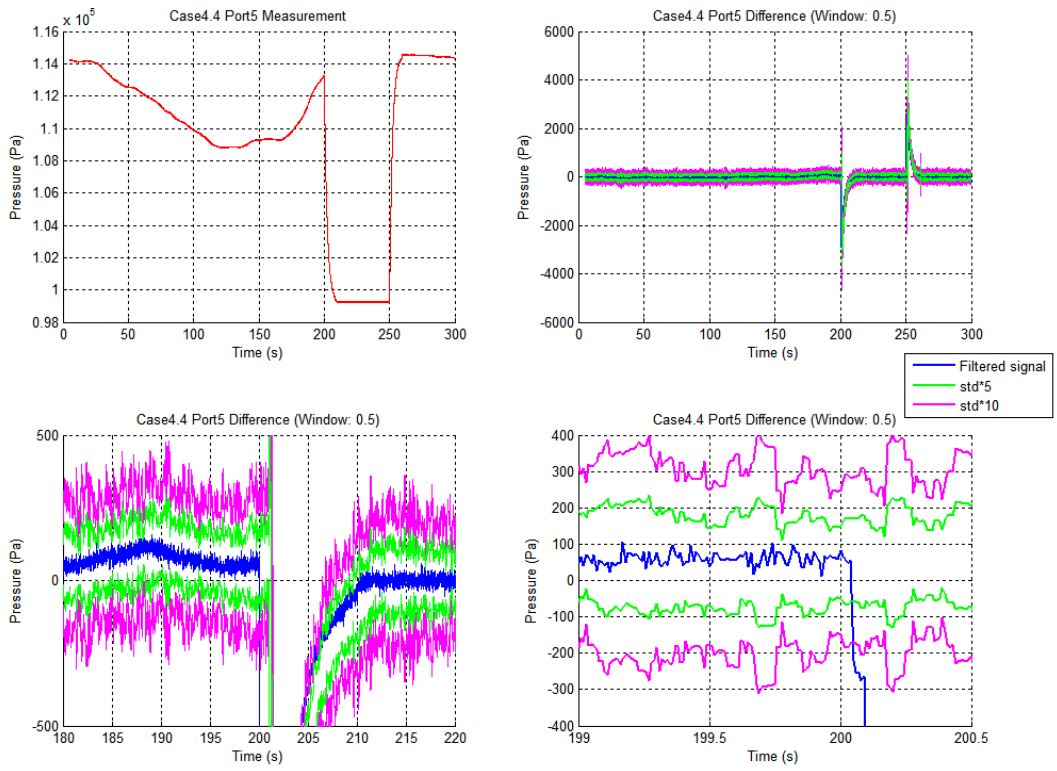

Figure 5.11: Case4.4: Thresholds and Fault Detection

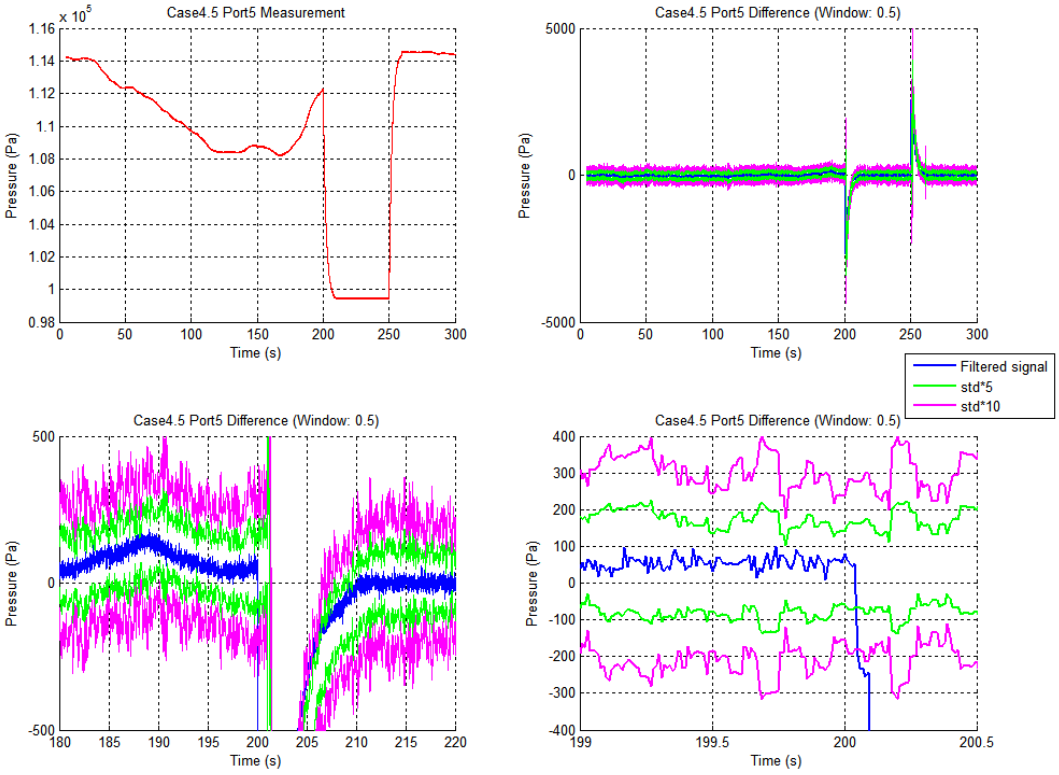

Figure 5.12: Case4.5: Thresholds and Fault Detection

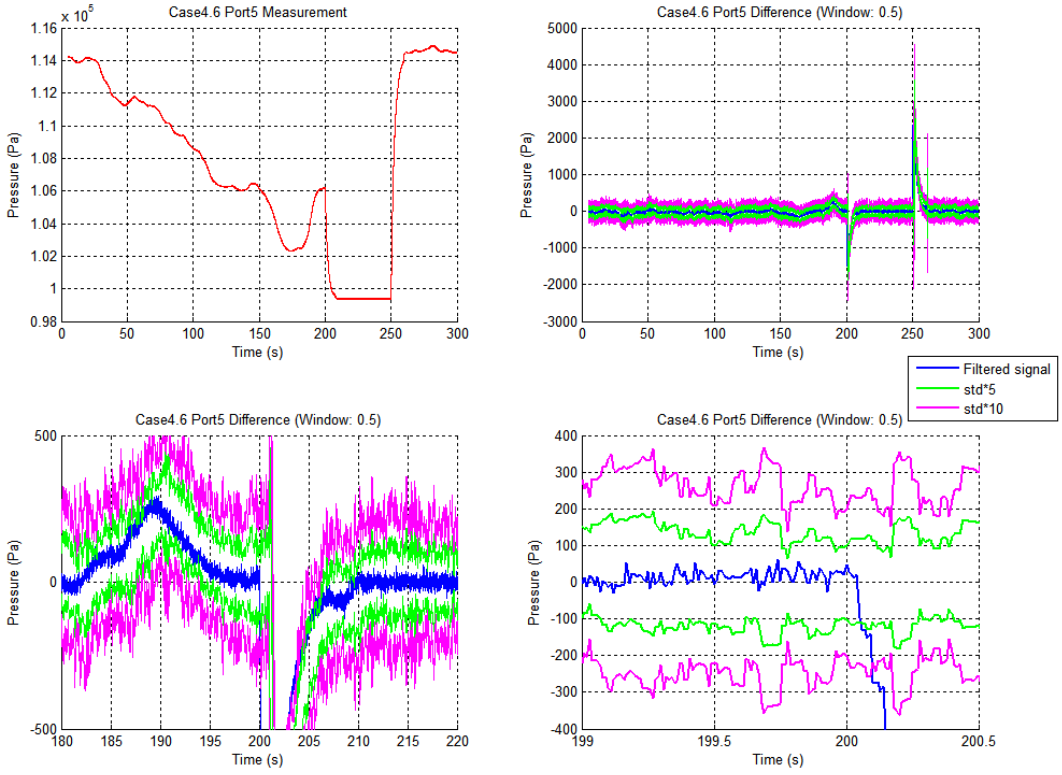

Figure 5.13: Case4.6: Thresholds and Fault Detection

5.3 Fault Accommodation Method

5.3.1 Method Selection

It is aimed to estimate air data from different sources like INS and GPS. Model based methods employ kinematic and dynamic relations for this adaptation. Classical model based approaches introduce pilot inputs to state equations. Force and momentum equations are used to model the aircraft motion. In this method, a well defined system model is required. Modeling uncertainties, unmodeled dynamics and disturbance inputs effect estimation results. On the other hand, kinematic equations do not involve control inputs. INS and GPS sensor outputs are processed through kinematic equations to estimate air data. Modeling errors and unknown disturbance inputs do not lead to any problem, but sensor accuracy is critical. As a result of these trade-offs, method selection for model based applications becomes problem specific. Kinematic relations based approach is more suitable for sensor FDA, whereas dynamic relations based methods are preferred for actuator FDA[16].

In this study, kinematic equations were used to eliminate modeling and disturbance related uncertainties. Following equations were used to generate a virtual air data sensor from INS and GPS outputs.

$$\begin{aligned}\dot{V} = g(-sin\theta\ cos\alpha\ cos\beta + sin\phi\ cos\theta\ sin\beta + cos\phi\ cos\theta\ sin\alpha\ cos\beta) + \\ A_x\ cos\alpha\ cos\beta + A_y\ sin\beta + A_z\ sin\alpha\ cos\beta\end{aligned} \tag{5.3}$$

$$\begin{aligned}\dot{\alpha} = g/(V\ cos\beta)(cos\phi\ cos\theta\ cos\alpha + sin\theta\ sin\alpha) + \\ 1/(V\ cos\beta)(A_z\ cos\alpha - A_x\ sin\alpha) + q - tan\beta(p\ cos\alpha + r\ sin\alpha)\end{aligned} \tag{5.4}$$

$$\begin{aligned}\dot{\beta} = g/V(sin\theta\ cos\alpha\ sin\beta + sin\phi\ cos\theta\ cos\beta - cos\phi\ cos\theta\ sin\alpha\ sin\beta) + \\ 1/V\ (-A_x\ cos\alpha\ sin\beta + A_y\ cos\beta - A_z\ sin\alpha\ sin\beta) + p\ sin\alpha - r\ cos\alpha\end{aligned} \tag{5.5}$$

$$\dot{\phi} = p + q\ sin\phi\ tan\theta\ + r\ cos\phi\ tan\theta \tag{5.6}$$

$$\dot{\theta} = q\ cos\phi - r\ sin\phi \tag{5.7}$$

$$\dot{\psi} = q\ (sin\phi/cos\theta\ ) + r\ (cos\phi/cos\theta\ ) \tag{5.8}$$

Ax, Ay and Az correspond to the measured specific forces in the center of gravity, g is the gravitational acceleration which is assumed to be constant and p, q and r are the rotational rates. [39, 40].

5.3.2 Kalman Filtering

Kalman filtering is an optimal and recursive state estimator of linear dynamic systems. For nonlinear systems, Extended Kalman Filter and Unscented Kalman Filter are used widely.

Extension to non-linear systems is achieved through linearization around the current mean estimate within the extended Kalman filter (EKF). Mean and covariance matrix of the state vector are updated through the first order linearized system model. [41]. This first-order approximation may introduce large errors as system nonlinearity increases and cause to sub-optimal performance of the filter. Contrary to the EKF, the unscented Kalman filter (UKF) use the nonlinear system model to propagate the state vector. The state distribution is taken as a Gaussian Random Variable, and this distribution is represented through a carefully selected sample points. Then, these sample points, i.e. sigma points, are propagated through the non-linear system model to obtain posterior mean and covariance matrix [42].

The Unscented Transform (UT) is a convenient way to compute the mean and variance of a random variable that undergoes a nonlinear transformation. Con-

sider a random variable x with mean $\bar{x}$ and covariance P_x, and it goes through a nonlinear function, $y = f(x)$. Then, $2L + 1$ sigma points,X, are generated through the following equations to represent GRV distribution of x , and to calculate the statistics of y[43].

$$X_0 = \bar{x} \tag{5.9}$$

$$X_i = \bar{x} + (\sqrt{(L + \lambda)\ P_x})_i\ i = 1, .., L \tag{5.10}$$

$$X_i = \bar{x} - (\sqrt{(L + \lambda)\ P_x})_{i-L}\ i = L + 1, .., 2L \tag{5.11}$$

$$W_0^{(m)} = \frac{\lambda}{(L + \lambda)} \tag{5.12}$$

$$W_0^{(c)} = \frac{\lambda}{(L + \lambda)} + (1 - \alpha^2 + \beta) \tag{5.13}$$

$$W_i^{(m)} = W_i^{(c)} = \frac{1}{2(L + \lambda)}\ i = 1, .., 2L \tag{5.14}$$

where

$$\lambda = \alpha^2\ (L + \kappa) - L$$

λ is used for scaling. The spread of the sigma points around the mean value is deterimned by α, it is usually taken as a small positive number. κ is a secondary scaling parameter and usually set to 0, and β indicates the prior knowledge of the distribution and is taken as 2 for Gaussian distributions. W_i are sigma point weights.

If a non-linear system equations are given as:

$$x_{k+1} = f_k(x_k) + w_k \tag{5.15}$$

$$y_k = h_k(x_k) + v_k \tag{5.16}$$

Following steps [43] are followed in Unscented Kalman Filter.

Initialize with:

$$\begin{aligned} \hat{x}_0 &= E(x_0) \\ P_0 &= E((x_0 - \hat{x}_0)(x_0 - \hat{x}_0)^T) \end{aligned} \tag{5.17}$$

For $k\epsilon\{1, .., \infty\}$, calculate sigma points:

$$X_{k-1} = [\hat{x}_{k-1} \quad \hat{x}_{k-1} + \gamma\sqrt{P_{k-1}} \quad \hat{x}_{k-1} - \gamma\sqrt{P_{k-1}}] \tag{5.18}$$

Time update equations:

$$X_{k|k-1} = F[X_{k-1}, u_{k-1}] \tag{5.19}$$

$$\hat{x}_k^- = \sum_{i=0}^{2L} W_i^{(m)} \, X_{i,k|k-1} \tag{5.20}$$

$$P_k^- = \sum_{i=0}^{2L} W_i^{(c)} [X_{i,k|k-1} - \hat{x}_k^-][X_{i,k|k-1} - \hat{x}_k^-]^T + R^v \tag{5.21}$$

$$Y_{k|k-1} = H[X_{k|k-1}] \tag{5.22}$$

$$\hat{y}_k^- = \sum_{i=0}^{2L} W_i^{(m)} \, Y_{i,k|k-1} \tag{5.23}$$

Measurement update equations:

$$P_{\bar{y}_k,\bar{y}_k} = \sum_{i=0}^{2L} W_i^{(c)} [Y_{i,k|k-1} - \hat{y}_k^-][Y_{i,k|k-1} - \hat{y}_k^-]^T + R^n \tag{5.24}$$

$$P_{x_k,y_k} = \sum_{i=0}^{2L} W_i^{(c)} \, [X_{i,k|k-1} - \hat{x}_k^-][Y_{i,k|k-1} - \hat{y}_k^-]^T \tag{5.25}$$

$$K_k = P_{x_k,y_k} P_{\bar{y}_k,\bar{y}_k}^{-1} \tag{5.26}$$

$$\hat{x}_k = \hat{x}_k^- + K_k(y_k - \hat{y}_k^-) \tag{5.27}$$

$$P_k = P_k^- - K_k P_{\bar{y}_k, \bar{y}_k} K_k^T \tag{5.28}$$

where $\gamma = \sqrt{(L + \lambda)}$, L: dimension of the state, R^v: process noise covariance, R^n: measurement noise covariance

CHAPTER 6

RESULTS AND DISCUSSION

FDA algorithm was tested under various conditions. First, no blockage scenario was tested to observe the healthy case. Then a scenario that no FDA algortihm was implemented to judge the critical role of FDA. Then one port blockage scenarios are tested to see the efficiency of the new calibration algorithm. Finally, more than one blockage is tested under time varying wind and turbulence conditions.

Port failures onset at 240 sec. and continue until the end of the simulation. In the graphs, 5hp usage time is given. If one port blockage is detected by the algorithm, redundant port coefficient is used. For example, if Port 1 is blocked, Port 3 coefficient, C_3 is used instead. Port coefficient usage times are also shown in the graphs. AOA, AOS and airspeed data is fed from 5hp model to autopilot. When more than one port blockage is detected, 5hp outputs are disregarded and air data is supplied from kinematic equations.

It is observed that algorithm detects the blockage quickly at every trial. In all the cases residuals were responsive to failures and disturbances were filtered out. No false alarm was observed. Only the effect of blockage is prominent in residual signals..

Extreme conditions were tried for time varying wind conditions. Even though, fault detection was accomplished. Residuals were insensitive to environmental effects and thresholds were set adaptively. No false alarm was given.

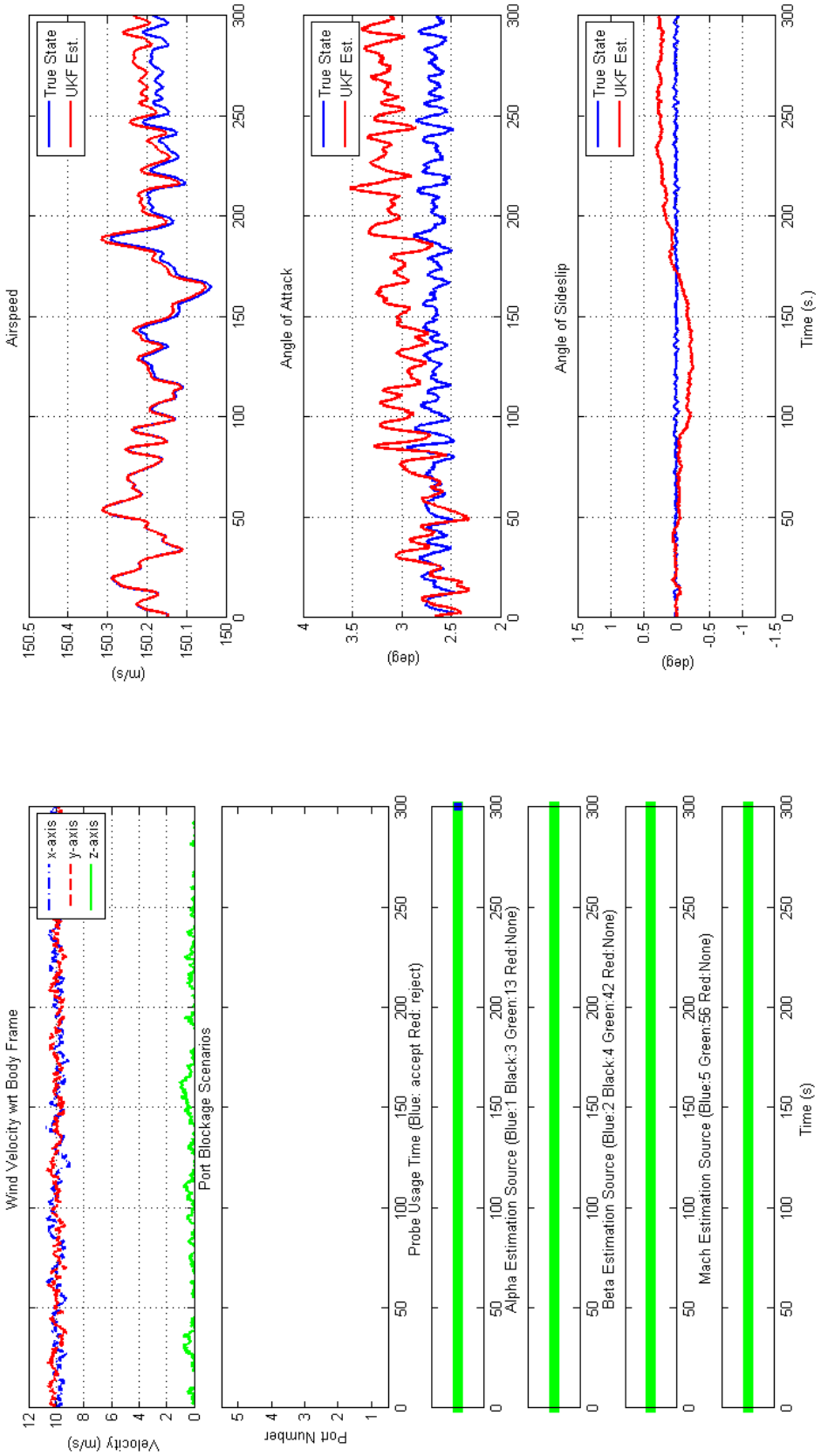

Figure 6.1: Scenario-1: No failure

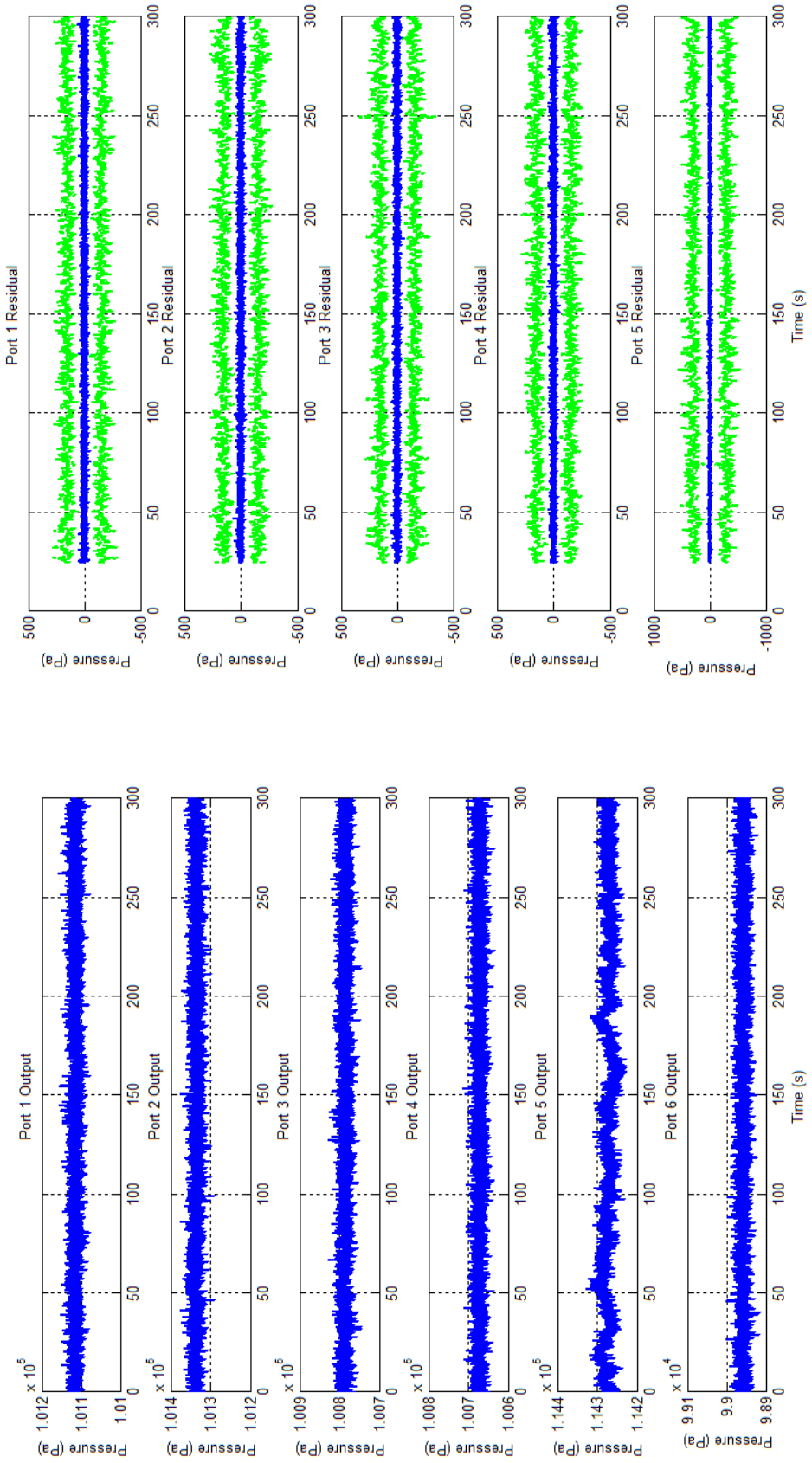

Figure 6.2: Scenario-1: No failure (cont'd)

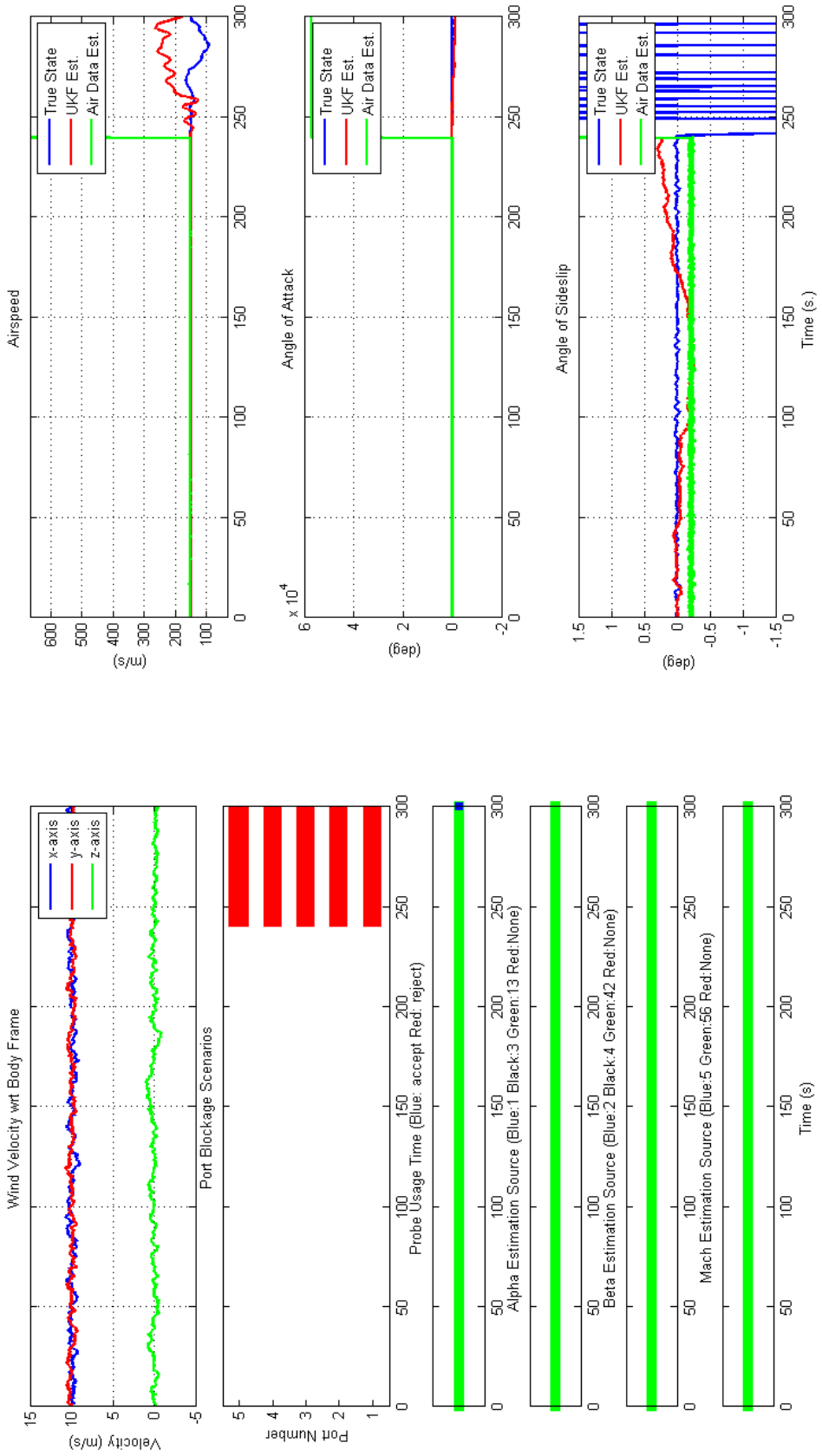

Figure 6.3: Scenario-2: Failure at 240 sec, No FDA

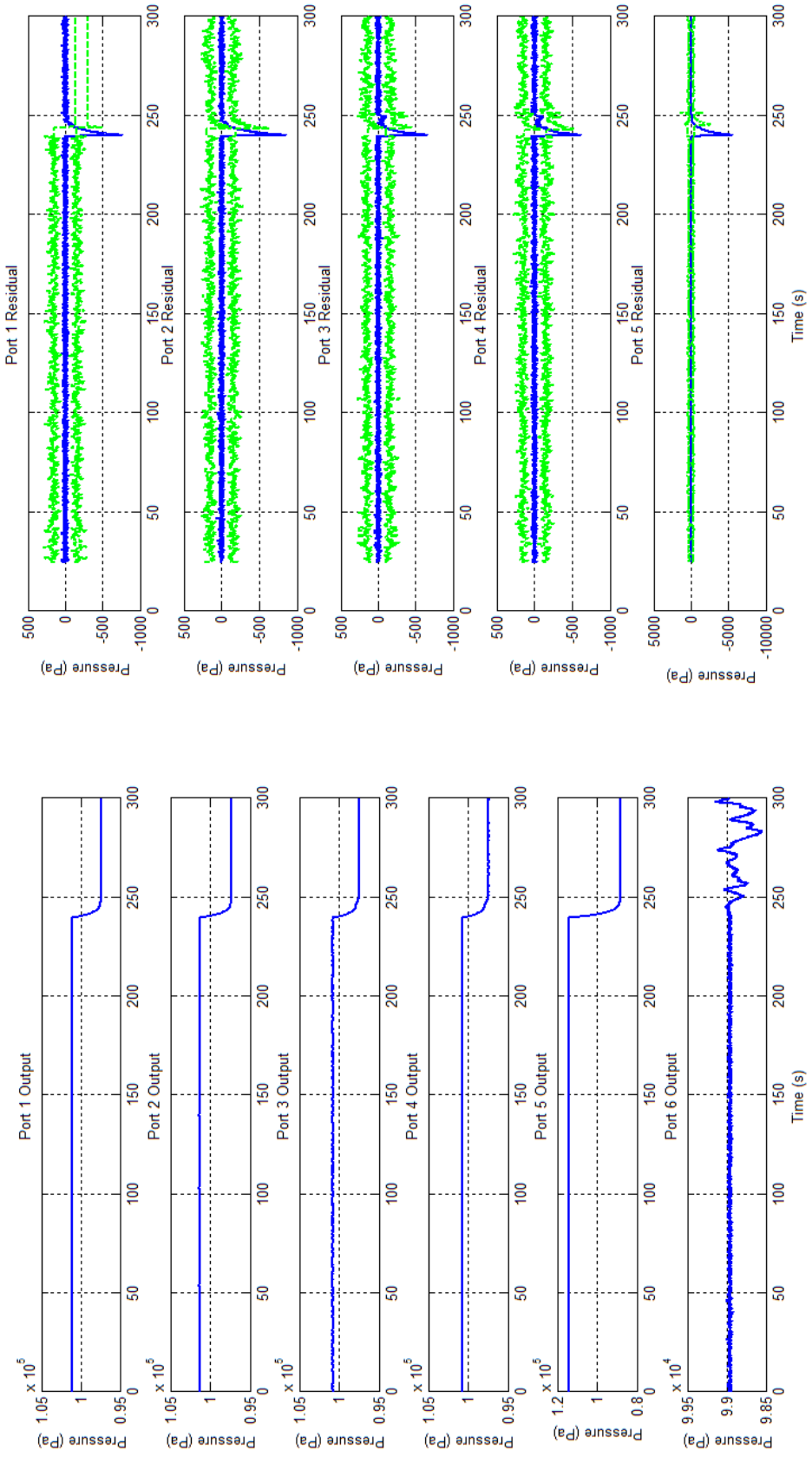

Figure 6.4: Scenario-2: Failure at 240 sec, No FDA (cont'd)

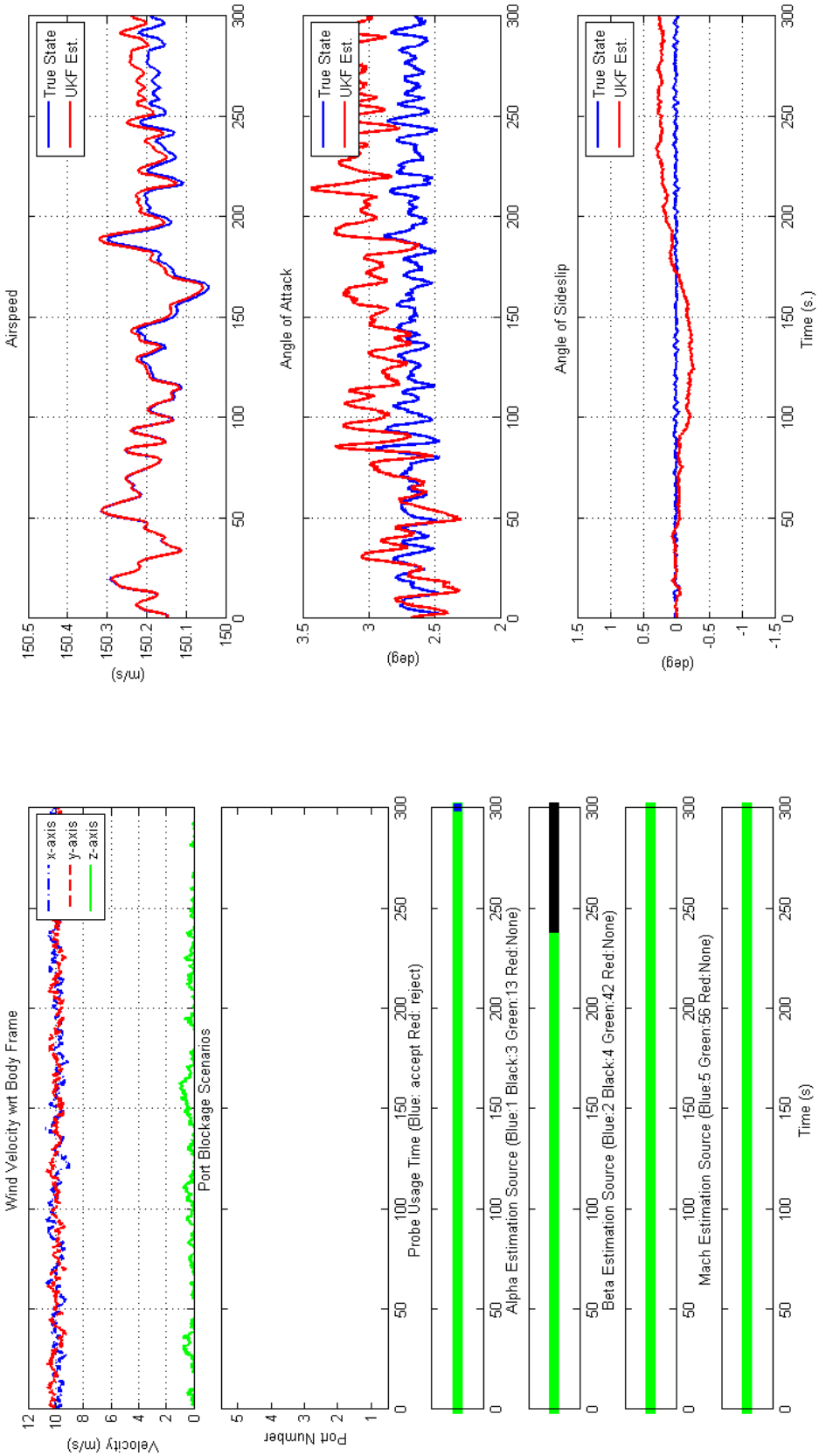

Figure 6.5: Scenario-3: Port-1 blockage with FDA

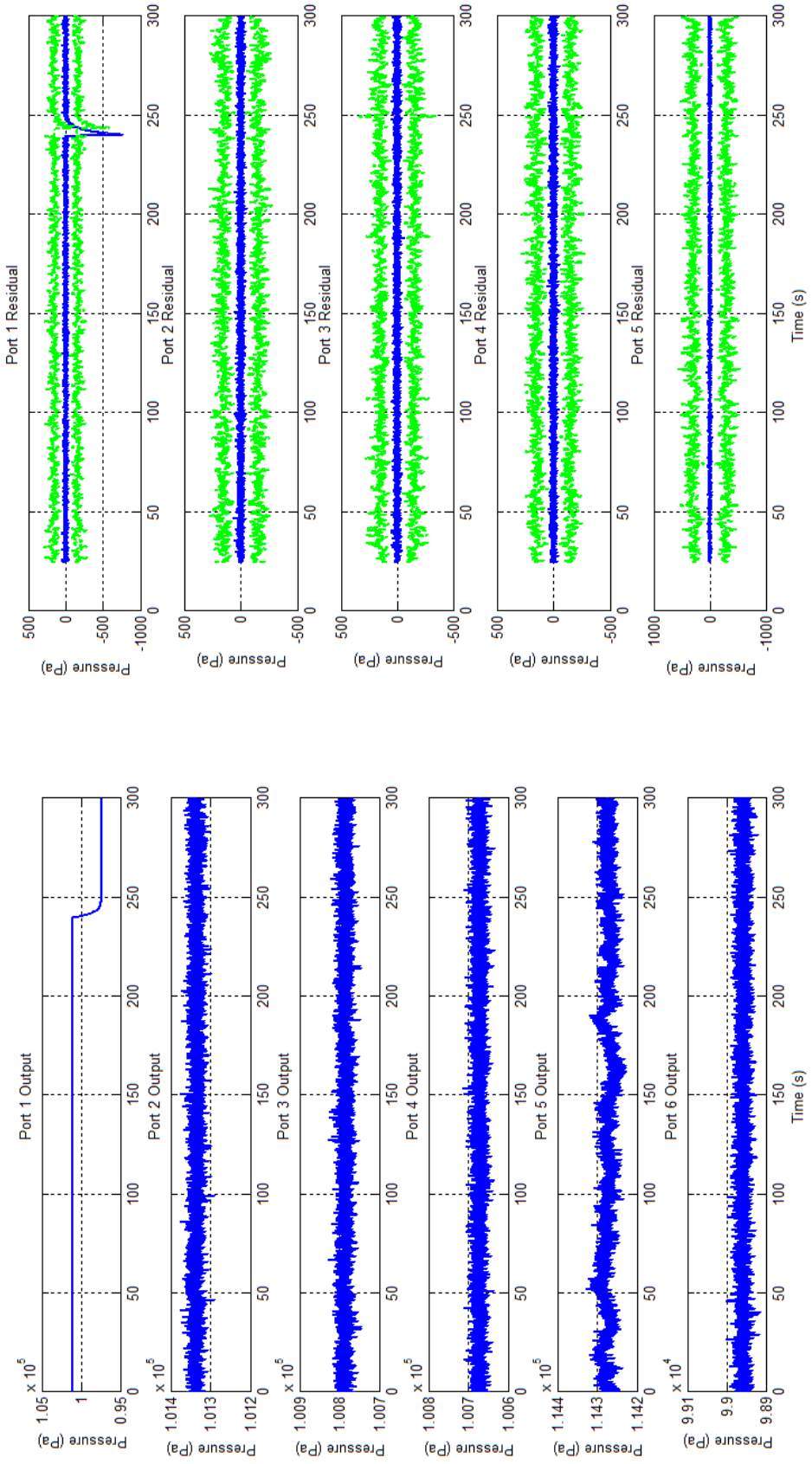

Figure 6.6: Scenario-3: Port-1 blockage with FDA (cont'd)

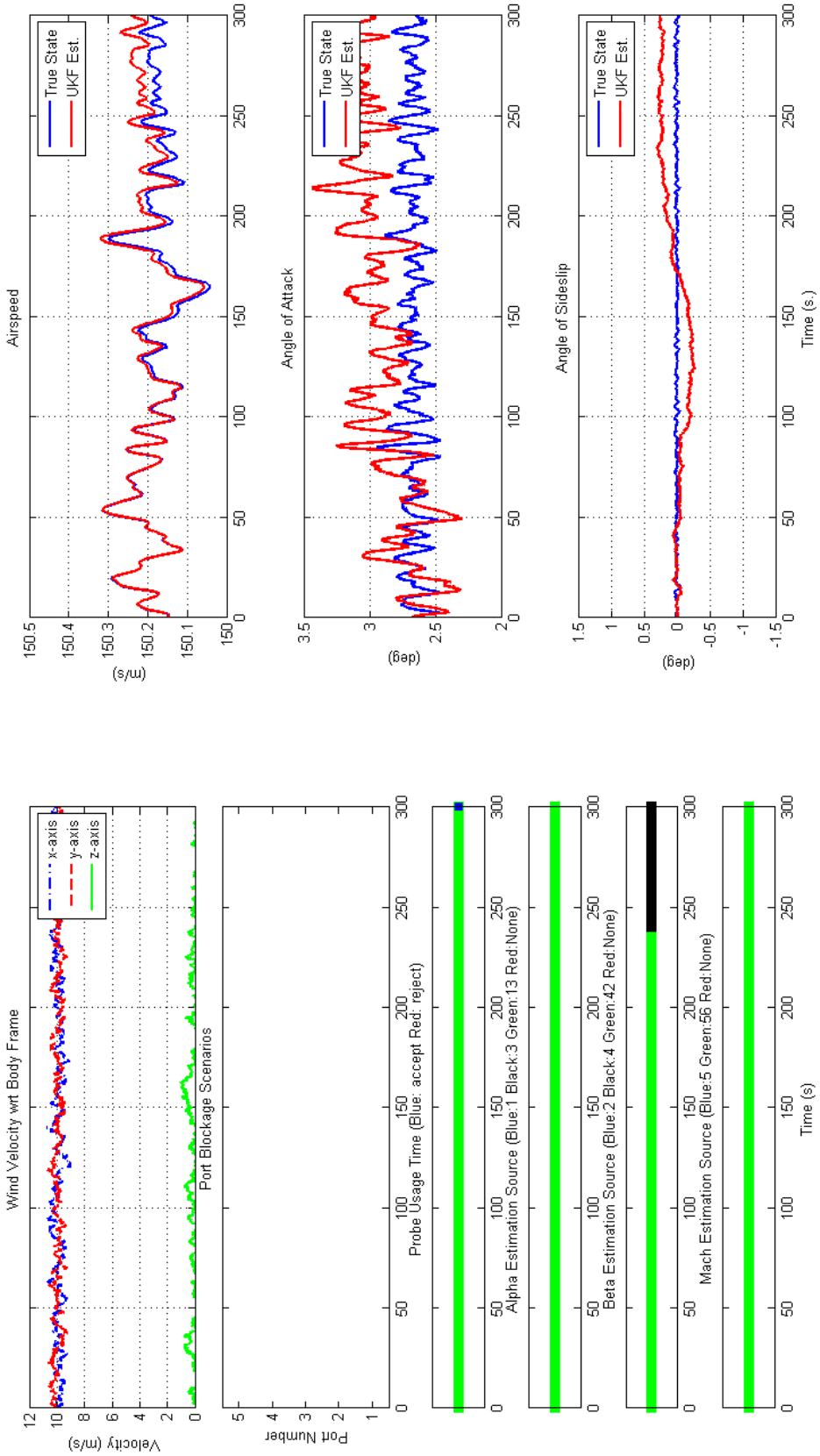

Figure 6.7: Scenario-4: Port-2 blockage with FDA

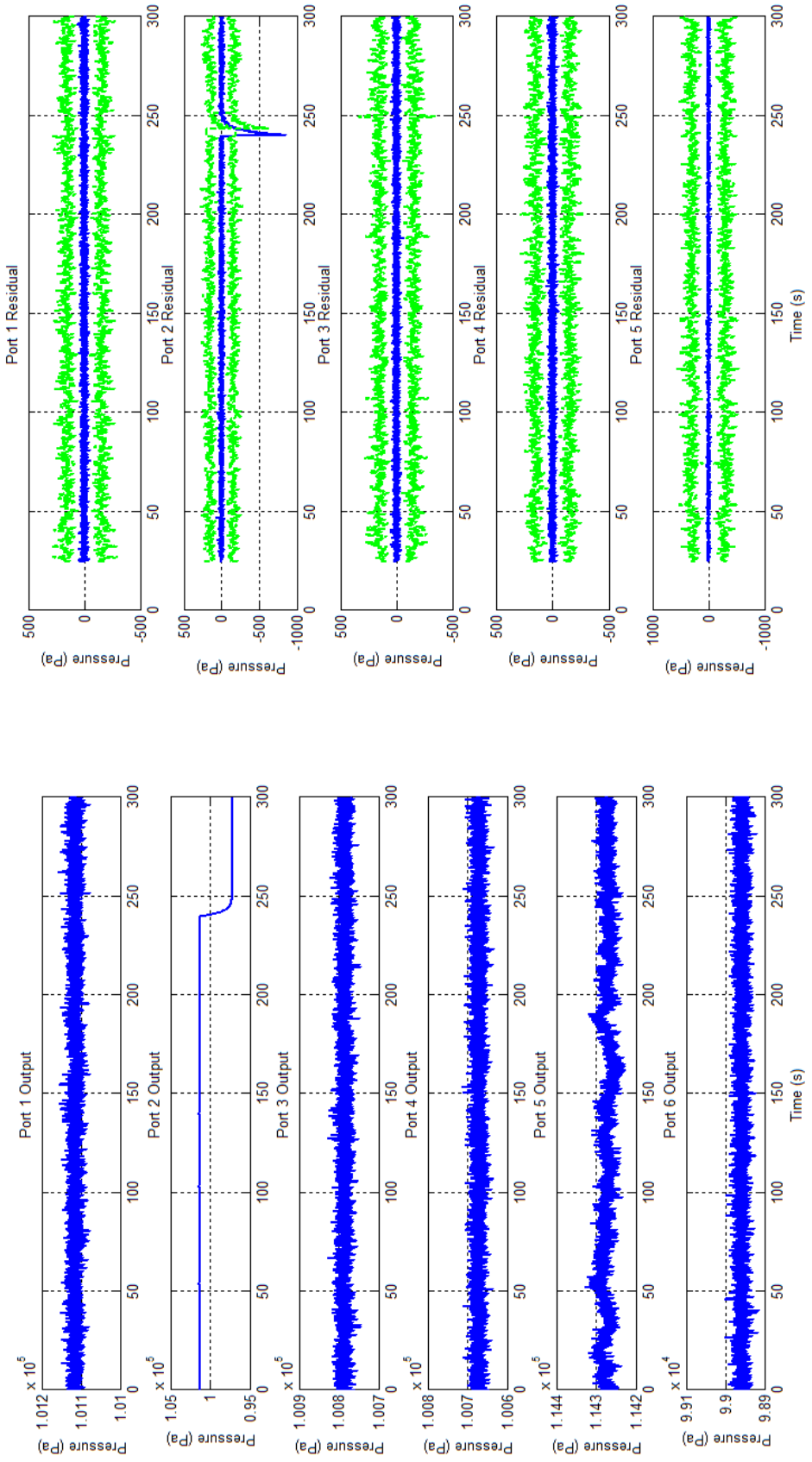

Figure 6.8: Scenario-4: Port-2 blockage with FDA (cont'd)

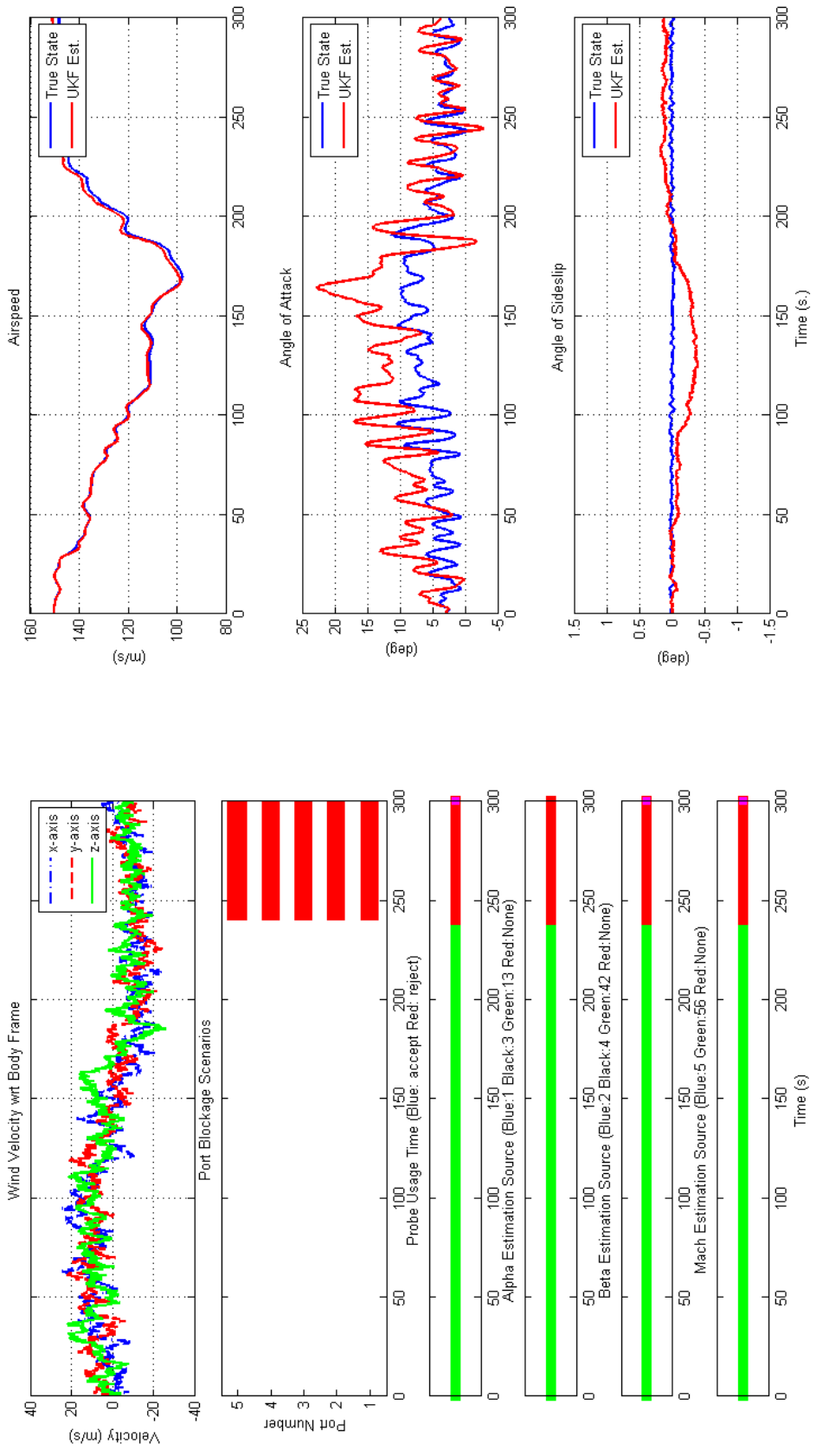

Figure 6.9: Scenario-5: Full blockage with FDA, Time varying wind, Severe turb.

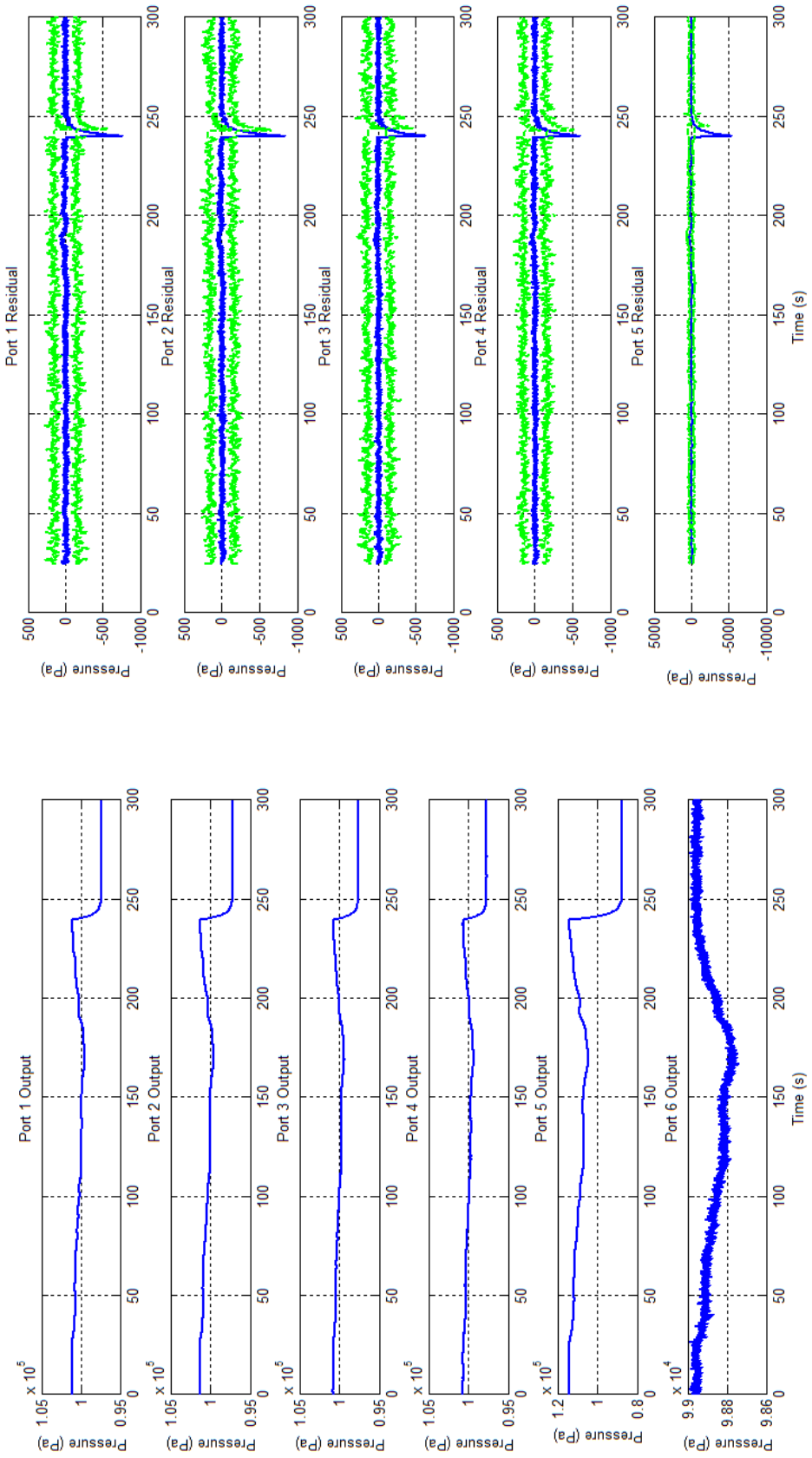

Figure 6.10: Scenario-5: Full blockage with FDA, Time varying wind, Severe turb. (cont'd)

Table6.1: FDA Algorithm Test Scenarios

Scenario	FDA	Wind (m/s)	Turbulence	Blocked port
1	No	Constant [10 10 0]	Light	No blockage
2	No	Constant [10 10 0]	Light	Full blockage
3	Yes	Constant [10 10 0]	Light	Port 1
4	Yes	Constant [10 10 0]	Light	Port 2
5	Yes	Time varying, Amp:30	Severe	Full blockage

CHAPTER 7

CONCLUSION

The aim of this thesis was to develop a fault detection and accommodation algorithm for air data systems during the level flight, in which pitot tube obstruction led to numerous fatal accidents. A simulation built in Simulink/Matlab environment which consists of 6 DOF Boeing 747 and five-hole-probe sensor model was used to conduct analysis. The model was consistent with the working principle of a five-hole probe. Wind tunnel test results for a five-hole probe were used to model pressure readings at 5 hole probe ports for different AOA, AOS and airspeed (Mach) values. Then, a calibration algorithm was applied to estimate air data. Port blockage was introduced as a sudden drop in pressure readings. A signal based fault detection and a model based fault accommodation algorithms were designed. These algorithms were verified and validated for different wind and turbulence conditions and Air France 447 accident scenario as well.

Initially, the basic information about the air data systems and five-hole probes were presented. The importance of air data for flight control and airspeed-dependent corrections such as altitude and temperature corrections were mentioned. Afterwards, the adequacy of industrial applications for fault detection and accommodation were evaluated. It was deduced from the accident scenarios that pitot failure does not cause an accident by itself. Following the pitot tube failure, autopilot disconnects and either the erroneous air data is displayed or no indication is given to flight crew. Exposure to unreliable airdata, indication and warnings, flight crew may react inappropriately and lead to a fatal accident.

It is essential to understand the distinct characteristics of failure mechanism.

Therefore, Air France 447 Accident (2009), which was caused by frozen pitot tubes in level flight, was studied in detail to comprehend the characteristics and consequences of an abrupt pitot tube failure.

Mainly two approaches exist for failure detection of pitot tubes; model based and signal based. Model based approaches create a virtual air data sensor. GPS and INS provide aircraft velocity and attitude information with respect to ground and aircraft body-axis, and with the knowledge of wind speed, it is possible to find out the airspeed. This airspeed is used as reference to monitor air data system health. Hence, wind data becomes critical for fault detection performance. Most of the approaches in literature use constant wind assumption or obtain wind data from another resource. In this study, the requirement of wind data is eliminated by implementing a signal based fault detection method. It was observed that frequency is a distinctive feature between blockage and disturbances. A sharp change in pressure data is observed when blockage occurs. Environmental factors such as wind and turbulence have lower frequency. This property is used for fault detection. Signal based monitoring is used and an online high pass filter is applied. Threshold is generated during the process adaptively. Light, medium and severe turbulence conditions with time varying wind profile were tested and fault detection was accomplished on each trial. Fault is detected at less than 0.5 seconds even at high wind and turbulence conditions with no false alarm. Early detection and isolation of erroneous data are very critical for flight safety. Figure 4.5 shows that, in Air France 447 flight, 4 seconds after the pitot tube failure, faulty air data was used in altitude corrections and altitude was indicated lower than the actual value. This false indication confused the pilots and led to inappropriate responses.

Simulation used in the analysis models the cruise flight of Boeing 747. Probe model was integrated. Pressure built up at each port to the corresponding air data was taken from lookup tables generated from wind tunnel data. Therefore, it is not suitable to simulate altitude variations or climbing period. However, to compare the rate of change of altitude related pressure variation and blockage related variation with high pass filter, a pressure drop was introduced at each port measurements. Static pressure difference corresponding to altitude change was

subtracted. It was an approximation and did not represent the true measured data, but in the scope of this analysis frequency was considered. Therefore, the rate of change is important, not the amount of change. Simulating probe with wind tunnel data is a restriction to evaluate the actual performance of the proposed FDA system. For future studies, five-hole probe pressure readings obtained from real flight data should be used.

A new algorithm was developed for five-hole probe calibration. The purpose was to enhance the operating region of five-hole probes. In case one of the head ports is blocked, the faulty measurement is eliminated from the rest of the calculations and 5hp continues to function properly. On the other hand, it is not possible to eliminate faulty input in traditional approaches. By virtue of this method, the operating range of 5hp is enhanced and flight incidence and Mach number are still available with good accuracy in case of any pressure-reading error.

REFERENCES

[1] Federal Aviation Administration lessons learned home. http://lessonslearned.faa.gov/ll_main.cfm?TabID=1&LLID=76&LLTypeID=14. Accessed: 2015-06-09.

[2] Wikipedia austral líneas aéreas flight 2553. https://en.wikipedia.org/wiki/Austral_L%C3%ADneas_A%C3%A9reas_Flight_2553. Accessed: 2015-06-12.

[3] Wikipedia birgenair flight 301. https://en.wikipedia.org/wiki/Birgenair_Flight_301#cite_note-1. Accessed: 2015-07-12.

[4] Fsf Editorial S F Editorial Staff. Erroneous Airspeed Indications Cited in Boeing 757 Control Loss. *FSF: Accident Prevention*, 56(10):1–8, 1999.

[5] Aviation Safety Network accident description. http://aviation-safety.net/database/record.php?id=19960206-0. Accessed: 2015-07-12.

[6] Wikipedia air france flight 447. https://en.wikipedia.org/wiki/Air_France_Flight_447. Accessed: 2015-06-09.

[7] Bureau d'Enquêtes et d'Analyses pour la sécurité de l'aviation civile. Final Report: On the accident on 1st June 2009 to the Airbus A330-203 registered F-GZCP operated by Air France flight AF 447 Rio de Janeiro - Paris. (June 2009), 2012.

[8] Skybrary b752, en-route, northern ghana, 2009 (loc). http://www.skybrary.aero/index.php/B752,_en-route,_Northern_Ghana,_2009_(LOC). Accessed: 2015-06-15.

[9] Sathya Silva and Roger K Nicholson. Categorization of Unreliable Airspeed Events Using Rasmussen's Human Performance Model. *International Congress of the Aeronautical Sciences*, 2012.

[10] Ali Zolghadri. Advanced model-based FDIR techniques for aerospace systems: Today challenges and opportunities. *Progress in Aerospace Sciences*, 53:18–29, 2012.

[11] R Isermann. Trends in the application of model based fault detection and diagnosis of technical processes. *Control Eng. Practice*, 5(5):709–719, 1997.

[12] M. M. Tousi and K. Khorasani. Robust observer-based fault diagnosis for an unmanned aerial vehicle. *2011 IEEE International Systems Conference, SysCon 2011 - Proceedings*, pages 428–434, 2011.

[13] P.P. Harihara, Kyusung Kim Kyusung Kim, and a.G. Parlos. Signal-based versus model-based fault diagnosis-a trade-off in complexity and performance. *4th IEEE International Symposium on Diagnostics for Electric Machines, Power Electronics and Drives, 2003. SDEMPED 2003.*, pages 24–26, 2003.

[14] R.J. Patton. Fault detection and diagnosis in aerospace systems using analytical redundancy. *Computing & Control Engineering Journal*, 2(3):127, 1991.

[15] R. Isermann. Supervision, fault-detection and fault-diagnosis methods - An introduction. *Control Engineering Practice*, 5(5):639–652, 1997.

[16] J. Marzat, H. Piet-Lahanier, F. Damongeot, and E. Walter. Model-based fault diagnosis for aerospace systems: a survey. *Proceedings of the Institution of Mechanical Engineers, Part G: Journal of Aerospace Engineering*, 226(10):1329–1360, 2012.

[17] M Basseville and I V Nikiforov. Detection of Abrupt Changes : Mich ‘ ele Basseville. *Change*, 2(4):729–730, 1993.

[18] Mario G Perhinschi, Marcello R Napolitano, Giampiero Campa, Brad Seanor, John Burken, and Richard Larson. An Adaptive Threshold Approach for the Design of an Actuator Failure Detection and Identification Scheme. 14(3):519–525, 2006.

[19] David M. Johnson. A review of fault management techniques used in safety-critical avionic systems. *Progress in Aerospace Sciences*, 32(5):415–431, 1996.

[20] Philippe Goupil, Josep Boada-bauxell, Andres Marcos, Emmanuel Cortet, Murray Kerr, and Hugo Costa. AIRBUS efforts towards advanced real-time Fault Diagnosis and Fault Tolerant Control. pages 3471–3476, 2014.

[21] M Sghairi, a De Bonneval, Y Crouzet, J Aubert, and P Brot. Challenges in Building Fault-Tolerant Flight Control System for a Civil Aircraft. *International Journal of Computer Science, IAENG*, 35(4):1–5, 2008.

[22] L.R. Tomlinson and R.E. Freeman. Signal selection and fault detection apparatus and method, January 20 1998. US Patent 5,710,776.

[23] M.D.W. McIntyre and D.L. Sebring. Integrated fault-tolerant air data inertial reference system, March 22 1994. US Patent 5,297,052.

[24] Aviation Safety Network accident description. `http://aviation-safety.net/database/record.php?id=20081127-0`. Accessed: 2015-07-22.

[25] Philippe Goupil. AIRBUS state of the art and practices on FDI and FTC in flight control system. *Control Engineering Practice*, 19(6):524–539, 2011.

[26] Venkat Venkatasubramanian, Raghunathan Rengaswamy, Kewen Yin, and Surya N. Kavuri. A review of process fault detection and diagnosis. *Computers & Chemical Engineering*, 27(3):293–311, 2003.

[27] Signal-based Approaches, Zhiwei Gao, Senior Member, Carlo Cecati, and Steven X Ding. A Survey of Fault Diagnosis and Fault-Tolerant Techniques — Part I : Fault Diagnosis With. 62(6):3757–3767, 2015.

[28] Zhiwei Gao, Senior Member, Carlo Cecati, and Steven X Ding. A Survey of Fault Diagnosis and Fault-Tolerant Techniques — Part II : Fault Diagnosis With Knowledge-Based and Hybrid / Active Approaches. 62(6):3768–3774, 2015.

[29] Sø ren Hansen, Mogens Blanke, and Jens Adrian. Diagnosis of UAV pitot tube defects using statistical change detection. *IFAC Proceedings Volumes (IFAC-PapersOnline)*, 7(PART 1):485–490, 2010.

[30] Shigeru Imai, Richard Klockowski, and Carlos A Varela. Self-Healing Spatio-Temporal Data Streams Using Error Signatures.

[31] M. L. Fravolini, Srikanth Gururajan, G. De Angelis, a. Moschitta, Haiyang Chao, and Marcello R. Napolitano. UAV Analytical Redundancy based fault detection of the airspeed sensor via generalized likelihood ratio test. *AIAA Guidance, Navigation, and Control (GNC) Conference*, pages 1–17, 2013.

[32] J. A. Lawford and K. R. Nippress. Calibration of air-data systems and flow direction sensors. Agard-ag-300, vol. 1, Sept. 1983.

[33] N Krause and J Dudzinsky. Flow -Direction Measurement with Fixed-Position Probes. *Nasa Technical Memorandum*, 1969.

[34] A. L. Treaster and A. M. Yocum. The calibration and application of five-hole probes. Technical report, ISA Transactions, 1979.

[35] Christian W. Wenger and William J. Devenport. Seven-hole pressure probe calibration method utilizing look-up error tables. *AIAA Journal*, 37(6):675–679, 1999.

[36] Tolga Yasa and Guillermo Paniagua. Robust procedure for multi-hole probe data processing. *Flow Measurement and Instrumentation*, 26(0):46 – 54, 2012.

[37] Jc Gonsalez. Five-hole Flow Angle Probe Calibration for the NASA Glenn Icing Research Tunnel. 1999.

[38] Sema Karahan and Ali T. Kutay. Calibration of Five-Hole Probe with Redundant Coefficients. 31st AIAA Aerodynamic Measurement Technology and Ground Testing Conference, AIAA Aviation.

[39] Brian L Stevens and Frank L Lewis. Aircraft Control and Simulation, 2003.

[40] L. Van Eykeren and Q.P. Chu. Sensor fault detection and isolation for aircraft control systems by kinematic relations. *Control Engineering Practice*, 31:200 – 210, 2014.

[41] Chuei Tin Chang and Jen Wen Chen. Implementation issues concerning the EKF-based fault diagnosis techniques. *Chemical Engineering Science*, 50(18):2861–2882, 1995.

[42] E a Wan and R Van Der Merwe. The unscented Kalman filter for nonlinear estimation. *Adaptive Systems for Signal Processing, Communications, and Control Symposium 2000. AS-SPCC. The IEEE 2000*, pages 153–158, 2002.

[43] E.A. A Wan and R. Van Der Merwe. The unscented Kalman filter for nonlinear estimation. *Technology*, v:153–158, 2000.

APPENDIX A

AIR FRANCE 447 FLIGHT DATA

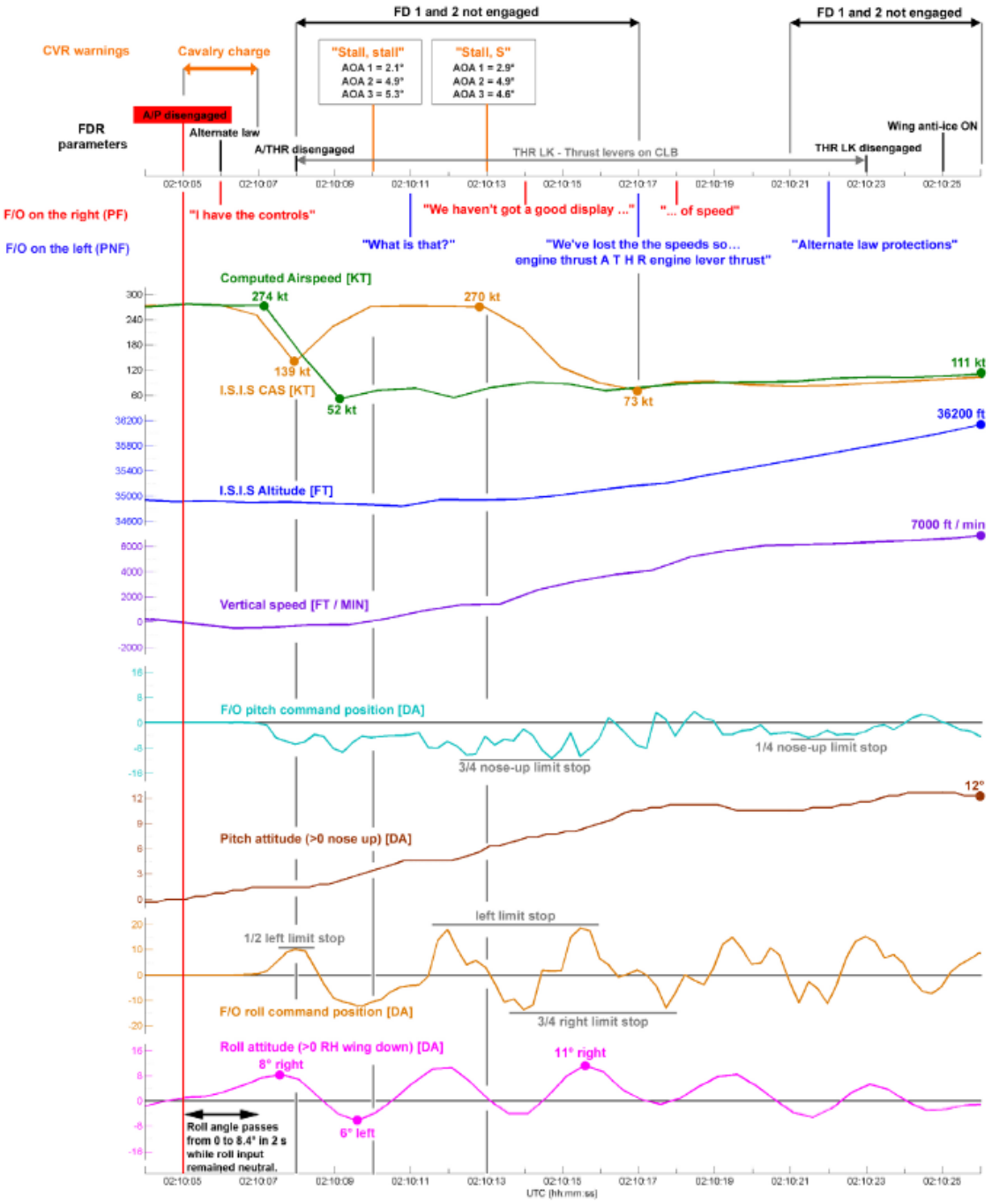

Figure .1: AF 447 Flight Parameters from 2 h 10 min 04 to 2 h 10 min 26 - BEA, "Final Report: On the accident on 1st June 2009 to the Airbus A330-203 registered F-GZCP operated by Air France flight AF 447 Rio de Janeiro - Paris",2012

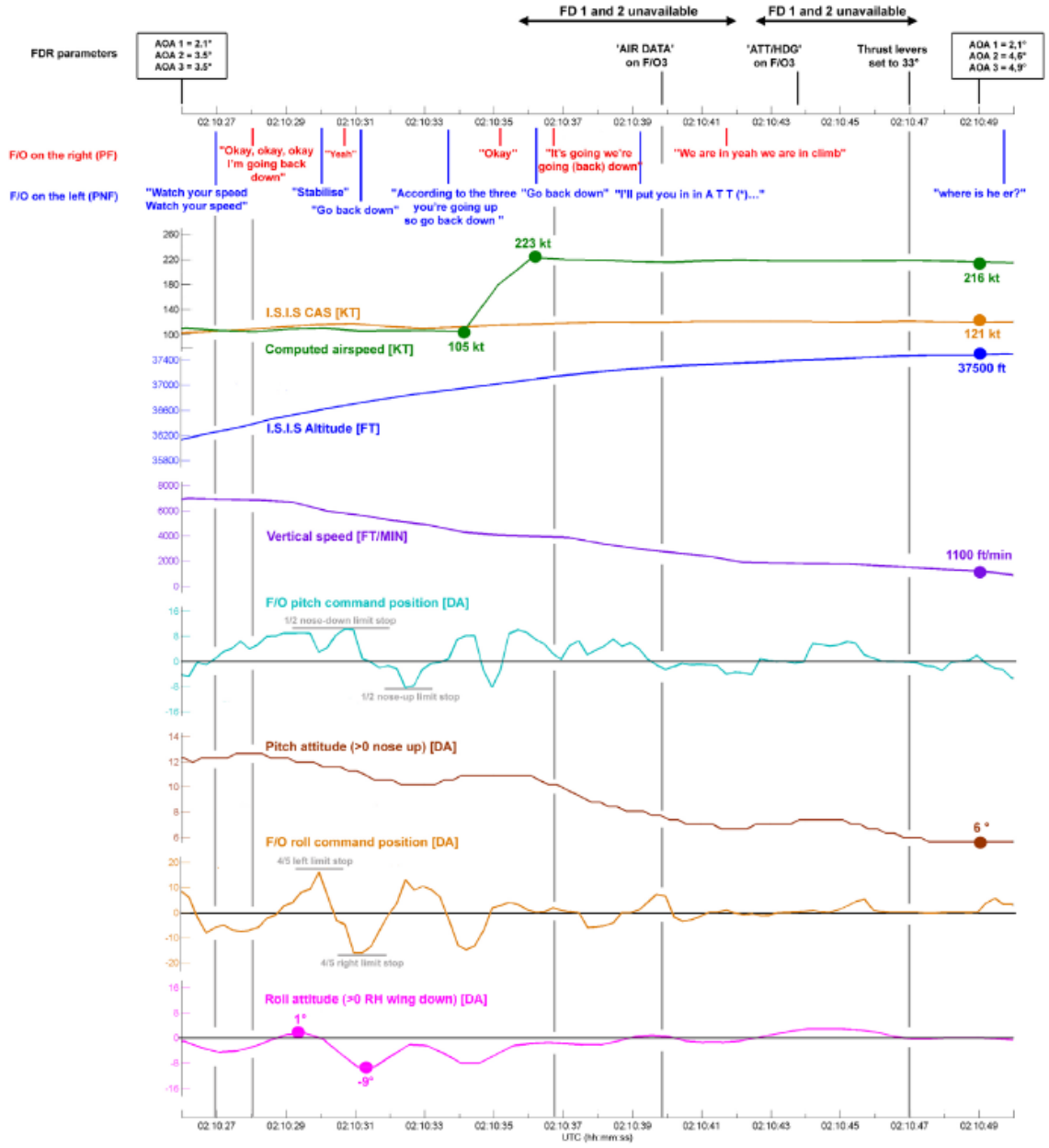

Figure .2: AF 447 Flight Parameters from 2 h 10 min 26 to 2 h 10 min 50 - BEA, "Final Report: On the accident on 1st June 2009 to the Airbus A330-203 registered F-GZCP operated by Air France flight AF 447 Rio de Janeiro - Paris",2012

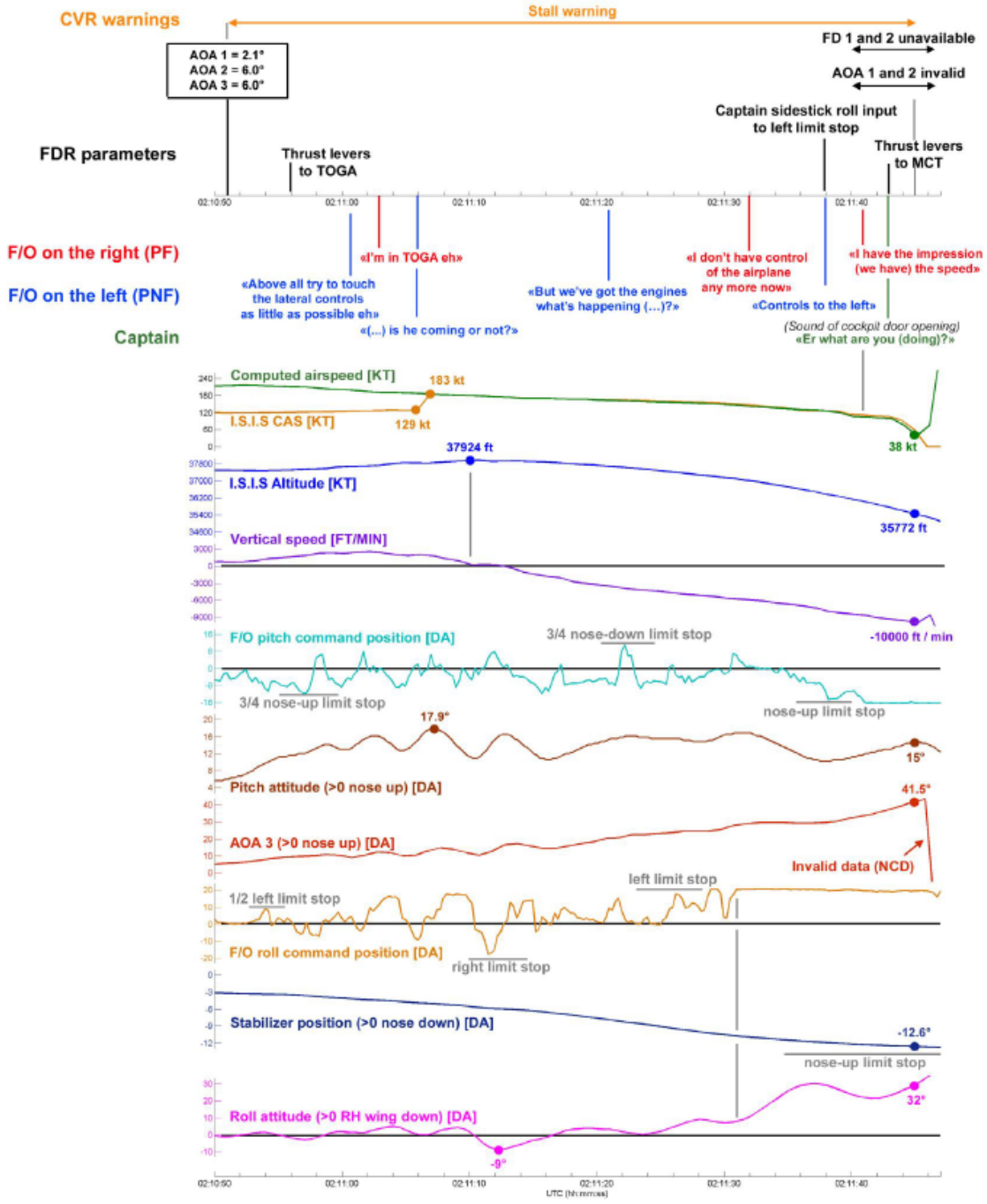

Figure .3: AF 447 Flight Parameters from 2 h 10 min 50 to 2 h 11 min 46 - BEA, "Final Report: On the accident on 1st June 2009 to the Airbus A330-203 registered F-GZCP operated by Air France flight AF 447 Rio de Janeiro - Paris",2012

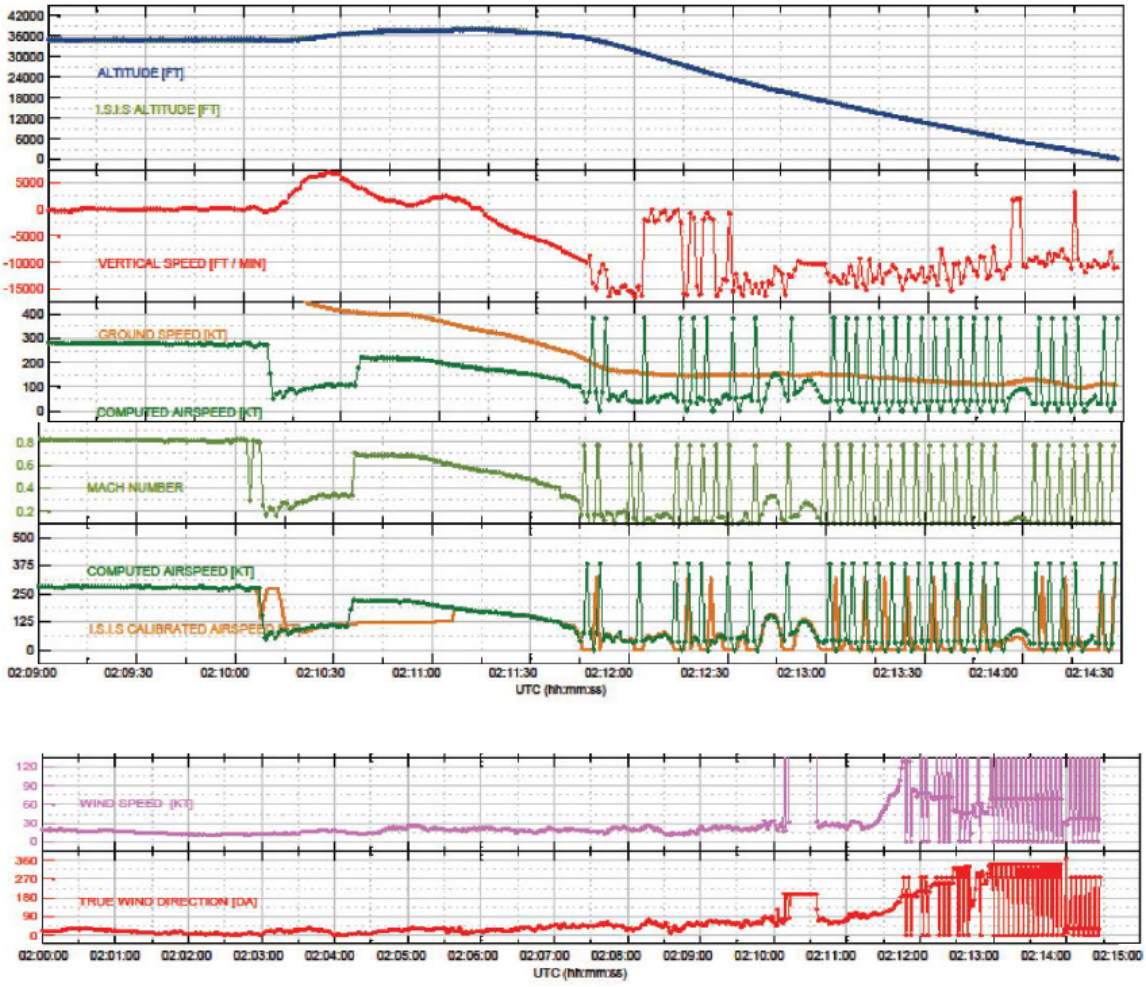

Figure .4: AF 447 Flight Parameters - BEA, "Final Report: On the accident on 1st June 2009 to the Airbus A330-203 registered F-GZCP operated by Air France flight AF 447 Rio de Janeiro - Paris",2012

Figure .5: ECAM displays after the pitot tubes failure - BEA, "Final Report: On the accident on 1st June 2009 to the Airbus A330-203 registered F-GZCP operated by Air France flight AF 447 Rio de Janeiro - Paris",2012